Nagra
Nationale
Genossenschaft
für die Lagerung
radioaktiver Abfälle

Cédra
Société coopérative
nationale
pour l'entreposage
de déchets radioactifs

Cisra
Società cooperativa
nazionale
per l'immagazzinamento
di scorie radioattive

TECHNICAL REPORT 89-17

REDUCTION SPHERES IN HEMATITIC ROCKS FROM NORTHERN SWITZERLAND: IMPLICATIONS FOR THE MOBILITY OF SOME RARE ELEMENTS

BEDA A. HOFMANN

NOVEMBER 1990

Mineralogisch-petrographisches Institut
der Universität Bern

Present address:
Naturhistorisches Museum, Bernastr. 15, 3005 Bern

Parkstrasse 23 5401 Baden/Schweiz Telephon 056/20 55 11

Nagra
Nationale
Genossenschaft
für die Lagerung
radioaktiver Abfälle

Cédra
Société coopérative
nationale
pour l'entreposage
de déchets radioactifs

Cisra
Società cooperativa
nazionale
per l'immagazzinamento
di scorie radioattive

TECHNICAL REPORT 89-17

REDUCTION SPHERES IN HEMATITIC ROCKS FROM NORTHERN SWITZERLAND: IMPLICATIONS FOR THE MOBILITY OF SOME RARE ELEMENTS

BEDA A. HOFMANN

NOVEMBER 1990

Mineralogisch-petrographisches Institut
der Universität Bern

Present address:
Naturhistorisches Museum, Bernastr. 15, 3005 Bern

Parkstrasse 23 5401 Baden/Schweiz Telephon 056/20 55 11

This report was prepared as an account of work sponsored by Nagra. The viewpoints presented and conclusions reached are those of the author and do not necessarily represent those of Nagra.

ABSTRACT

Reduction spheres are small-scale, isolated redox systems occurring in hematite-stained rocks of variable age, origin and provenience. Reduction spheres from Permotriassic continental red beds and from basement rocks of Northern Switzerland have been studied mineralogically and geochemically. More than 40 authigenic minerals occur in the dark, mineralized cores of the spheres. The most common minerals are roscoelite, uraninite and nickel arsenides, but minerals containing the precious metals Ag, Au, Pd and Pt, selenides and REE-rich uraninite have been found as well. The bleached spheres are depleted in ferric iron due to hematite dissolution. Mass balance calculations show that only a minor part of the trace elements present in the bulk rock has been mobilized during halo formation. The relative mobilities are: As>U>Ni>V. The elements precipitated as ore minerals in reduction sphere cores were probably released from iron hydroxides during their alteration to hematite. The red beds which contain reduction halos are unusually rich in As (100 ppm) compared with underlying reduced beds containing less than 5 ppm As. Reduction halo formation took place during the Mesozoic at depths of burial of 500 to 1'100 m. The porewaters were highly saline. Organic matter of unknown origin reacted with dissolved high-valence ions and hematite at discrete, randomly distributed sites in the rocks and caused local precipitation of rare elements as ore minerals and dissolution of hematite. Element migration was diffusive. Oxidation of organic matter and ore mineral precipitation was probably catalyzed by bacteria because the sulfides were formed by in situ low-temperature (< 100°C) sulfate reduction. Reduction spheres can be used to date and trace quantitatively element mobilities during red bed diagenesis. The geological significance of their presence is not yet understood.

Reduction spheres give qualitative information on element mobilities in an environment similar to that of a possible radioactive waste repository in Northern Switzerland. Diffusive element transport of U, REE, Pd and many other elements under oxidizing conditions is evidenced as well as immobilization of these elements by very local reducing conditions. Very high concentration gradients of U and other elements at redox boundaries persisted for roughly 10^8 years.

RÉSUMÉ

Les sphères de réduction sont de petits systèmes rédox isolés apparaîssant dans des roches tachetées d'hématites d'âges, d'origines et de provenances variables. Des sphères de réduction des couches rouges du permo-triassique continental ainsi que du socle rocheux du Nord de la Suisse ont été étudiées sur le plan minéralogique et géochimique. Plus de 40 minéraux autigènes apparaissent dans les sombres coeurs minéralisés de ces sphères. Les minéraux les plus communs sont roscoelite, uraninite et des arséniures de nickel, mais on a également trouvé des minéraux contenant les métaux précieux Ag, Au, Pd et Pt ainsi que des séléniures et des uraninites riches en terres rares. Les sphères lixiviées sont appauvries en ions ferritiques en raison de la dissolution de l'hématite. Des calculs de bilans de masses montrent que seule une très faible partie des éléments traces présents dans la masse rocheuse a été mobilisée durant la formation du halo. Les mobilités relatives sont: As>U>Ni>V. Les éléments précipités sous forme de minerais dans le coeur des sphères de réduction ont probablement été relâchés d'hydroxydes de fer lors de leur altération en hématite. Les couches rouges contenant des halos de réduction sont généralement riches en As (100 ppm) par rapport aux couches sous-jacentes réduites contenant moins de 5 ppm d'As. La formation des halos de réduction a eu lieu durant le Mésozoïque à des profondeurs de 500 à 1'100 m. Les eaux intersticielles étaient fortement salines. Des matières organiques d'origine inconnue ont réagi avec des ions dissous de haute valence et de l'hématite en des points discrets distribués au hasard dans les roches et ont causé la précipitation locale d'éléments rares sous forme de minerais ainsi que la dissolution de l'hématite. La migration des éléments fut diffusive. L'oxydation des matières organiques et la précipitation de minerais ont probablement été catalysées par des bactéries, les sulfures ayant été formés par la réduction in situ à basse température (<100°C) de sulfates. Les sphères de réduction peuvent être utilisées pour dater et situer quantitativement les mobilités des éléments durant la diagenèse des couches rouges. La signification géologique de leur présence n'est pas encore comprise.

Les sphères de réduction livrent des informations qualitatives sur les mobilités des divers éléments dans un environnement similaire à celui d'un éventuel dépôt final pour déchets radioactifs dans le Nord de la Suisse. Le transport diffusif d'U, de terres rares, de Pd et de bien d'autres éléments sous conditions oxydantes est évident de même que leur immobilisation due à des conditions réductrices extrêmement locales. De très fortes concentrations de gradients d'U et d'autres éléments aux frontières rédox se sont maintenues durant 10^8 années approximativement.

ZUSAMMENFASSUNG

Reduktionshöfe sind kleinräumige, isolierte Redoxsysteme, die in mit Hämatit durchwachsenen Gesteinen unterschiedlichen Alters und Ursprungs vorkommen. Die Reduktionshöfe von permotriassischen kontinentalen Rotschichten und vom Grundgebirge der Nordschweiz wurden sowohl mineralogisch als auch geochemisch untersucht. Mehr als 40 authigene Mineralien sind in den dunklen, mineralisierten Kernen der Höfe erkennbar. Die häufigsten sind Roscoelith, Uraninit und Nickel-Arsenide; ausserdem wurden Mineralien gefunden, welche die Edelmetalle Ag, Au, Pd und Pt enthalten sowie Selenide und Uraninit, welcher reich an Seltenen Erden ist. Da Hämatit bevorzugt in Lösung geht, sind die ausgelaugten Höfe arm an Eisen (III). Massenbilanz-Berechnungen zeigen, dass nur ein geringer Teil der im Gestein vorhandenen Spurenelemente während der Hofbildung mobilisiert wurde. Die relativen Mobilitäten sind: As>U>Ni>V. Die Elemente, die als Erzmineralien in den Hofkernen ausfallen, wurden wahrscheinlich während der Umwandlung von Eisenhydroxiden zu Hämatit freigesetzt. Die Rotschichten, in denen Reduktionshöfe vorhanden sind, sind aussergewöhnlich arsenreich (100 ppm), im Vergleich zu den darunterliegenden reduzierten Schichten, die weniger als 5 ppm As enthalten. Die Bildung der Reduktionshöfe fand im Mesozoikum statt, in einer Tiefe von 500 bis 1'100 m. Die Porenwässer waren von hoher Salinität. An diskreten, unsystematisch verteilten Punkten in den Gesteinen reagierten organische Stoffe unbekannter Herkunft mit den gelösten Ionen hoher Wertigkeit und mit Hämatit, was zur lokalen Ausfällung von Seltenen Erden als Erzmineralien sowie Auflösung von Hämatit führte. Die Wanderung der Elemente erfolgte durch Diffusion. Die Oxidation organischer Stoffe und die Ausfällung der Erzmineralien wurden wahrscheinlich durch Bakterien katalysiert, weil die Sulfide durch eine Sulfatreduktion bei einer in-situ niedrigen Temperatur von < 100°C entstanden. Reduktionshöfe können zur quantitativen Datierung und Identifizierung der Mobilität verschiedener Elemente während der Diagenese der Rotschichten genutzt werden. Die geologische Bedeutung der Höfe ist noch nicht klar.

Reduktionshöfe liefern qualitative Information zur Mobilität verschiedener Elemente in einem Milieu, das der Umgebung eines potentiellen Endlagers in der Nordschweiz sehr ähnlich ist. Der diffuse Transport von U, Seltenen Erden, Pd und vielen anderen Elementen unter oxidierenden Bedingungen sowie die Immobilisierung dieser Elemente unter sehr lokal reduzierenden Bedingungen, können nachgewiesen werden. Sehr hohe Konzentrationsgradienten für U und andere Elemente an Redox-Grenzen blieben etwa 10^8 Jahre erhalten.

LIST OF CONTENTS

LIST OF FIGURES

LIST OF TABLES

1 INTRODUCTION

Reduction spheres are mm- to dm-sized, spherical or spheroidal structures found in continental red beds (Fig. 1 and 2), radiolarian cherts and in hematitic, altered crystalline rocks. Reduction spheres are devoid of iron oxide pigment. In their center, a dark core containing ore minerals and/or organic matter is common but not ubiquitous. Typical elements concentrated in reduction sphere cores are V, U, Ni, Co, As, Cu, Se, Pb and S, but many other elements have been found. Reduction spheres do not appear to have formed around detrital particles.

Although there is an extensive literature on reduction spheres, there is little consensus among authors about the processes leading to their formation. In no case the nature and the origin of the reductant could be explained satisfactorily. Reduction spheres contain multielement accumulations that are similar in many ways to roll-front-, unconformity-type- and vein-type Co-Ni-Bi-Ag-U deposits. In this paper, reduction spheres from Northern Switzerland will be described and genetic models will be discussed and compared with models proposed by other authors.

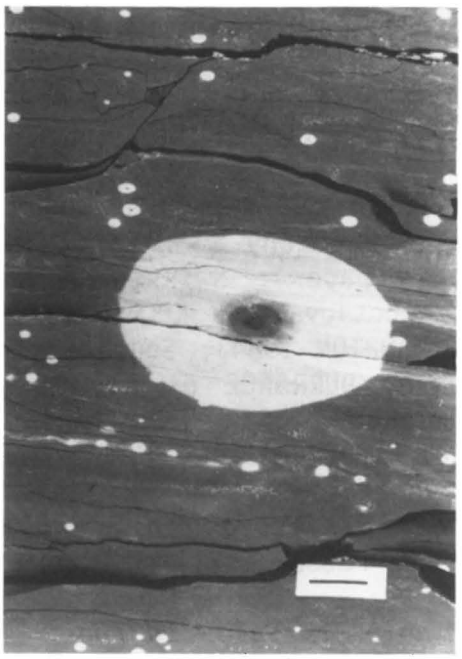

Fig. 1: Reduction spheres in clay-rich sandstone.
Riniken well 836.75 m. Scale bar = 1 cm.

Fig. 2: One large and several small reduction spheres in clay. Kaisten well, 226.95 m. Scale bar = 1 cm.

Reduction spheres have been described as fish eyes, reduction haloes, reduction spots, reduction mottling, bleaching haloes, (radioactive) concretions, (radioactive) nodules. These terms characterize the same phenomenon at different scales or proportions of spheres to cores. In this paper, the term "reduction sphere" will be used as it is most concise.

Reduction spheres have been described from continental red beds of late Proterozoic, Devonian, Carboniferous, Permian and Triassic age. Most of the occurrences are in Permian red beds. The known occurrences are briefly listed below:

Crystalline rocks: Altered Permian volcanics in the Saar-Nahe trough in Germany (EICHHOFF & REINECK 1952); altered lamprophyre, gneiss and granite in Northern Switzerland (HOFMANN 1986, this paper); altered felsic volcanics and granite, Black Forest, S Germany (this paper).

Proterozoic sediments: Nipigon, Ontario, Canada (TANTON 1948).

Cambrian to Silurian red slates of deep marine origin: Pennsylvania, New York and Vermont (DALE 1899, MILLER 1910, BEUTNER & CHARLES 1985).

Devonian red beds: Northern Scotland UK (PARNELL 1985, PARNELL & EAKIN 1987); East Greenland (authors observation, 1984).

Carboniferous red beds: New Brunswick and Nova Scotia, Canada (VAN DE POLL & SUTHERLAND 1976, DYCK & MCCORKELL 1983); Germany (MEMPEL 1960).

Permian red beds: Saar-Nahe, Germany (EICHHOFF & REINECK 1952, MEMPEL 1960); Saxony (SCHREITER 1930); Northern Switzerland (HOFMANN 1986, this paper); Swiss Alps (authors observation, 1988); NE Bohemia, Czechoslovakia (SKOCEK 1967); Warwickshire, UK (PONSFORD 1954, MYAKURA & HAMPTON 1984); South Devon, UK (CARTER 1931, PERUTZ 1940, HARRISON 1975, DURRANCE et al. 1978); Northern Ireland, UK (PARNELL 1988); Oklahoma, USA (HILL 1954, CURIALE et al. 1983); North Texas, USA (PIERCE et al. 1964).

Lower Triassic red beds: Northern Germany (SCHREITER 1932, MEMPEL 1960, FESSER 1971), Northern Switzerland (HOFMANN 1986).

Middle Triassic red beds: East Greenland (PERCH-NIELSEN et al. 1975, HOFMANN 1986); Salzuflen, Germany (MEMPEL 1960); Swiss Alps (FREY et al. 1980), Colorado Plateau (authors observation, 1988).

Late Jurassic to early Cretaceous radiolarian cherts: Warah-Formation of Oman (PETERS TJ. pers. comm. 1987).

2 GEOLOGY OF REDUCTION SPHERE OCCURRENCES IN NORTHERN SWITZERLAND

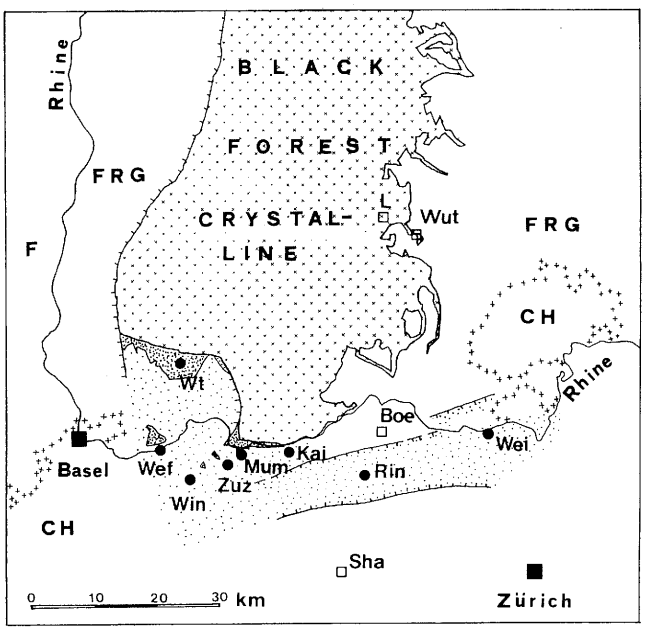

Fig. 3: Map of Northern Switzerland - Southwest Germany showing location of wells and outcrops discussed. Kai = Kaisten well, Wei = Weiach well, Rin = Riniken well, Boe = Boettstein well, Wef = Weierfeld well, Zuz = Zuzgen well, Wut = Upper Wutach valley, L = Lenzkirch, Wt = Weitenau, Mum = Mumpf. Densely rastered areas: Outcrops of Permian red beds. Loosely rastered area: Subcrop of Permian red beds (after DIEBOLD 1987).

2.1 Crystalline basement

Much like the nearby Black Forest massif in Southern Germany, the Northern Swiss crystalline basement is composed of migmatic gneisses, syn- and posttectonic Hercynian granites and posttectonic acid dykes of Late Carboniferous/Early Permian age. Lamprophyre dykes are quite common. The latest metamorphism affected the basement during the Hercynian orogenesis. During the late Caboniferous and the Permian, the basement has been uplifted and hydrothermally altered. During the Mesozoic, about 1'000 m of epicontinental sediments have been laid down on the basement and still cover much of the Crystalline in Northern Switzerland.

Occurrences of reduction spheres are restricted to strongly altered and usually cataclastic zones in the crystalline basement of the Kaisten, Leuggern and Schafisheim wells. Host rocks are gneisses, granites and lamprophyre dykes. With the exception of a Schafisheim sample (480 m below top of crystalline), all occurrences are in the topmost 100 m of the basement.

Similar occurrences of reduction spheres in altered crystalline rocks have been found in the Black Forest (S Germany). At Wittichen (Northern Black Forest), reduction spheres occur in an illitic fault gouge associated with a hydrothermal vein-type ore deposit of the Co-Ni-Bi-Ag-U-type. Near Lenzkirch, reduction spheres were found in an altered quartz porphyry dyke. Both occurrences are situated about 200 m below the top of the crystalline basement.

2.2 Permian red beds

Continental Permian red beds are common in and near a Permocarboniferous graben in Northern Switzerland (MÜLLER et al. 1984, MATTER 1987, LAUBSCHER 1987). Permian red beds were found in several drillholes (Rheinfelden, Wintersingen, Zuzgen, Weiach, Riniken, Kaisten). Surface exposures have been investigated at Mumpf (Northern Switzerland) and in Weitenau (FRG). Fanglomerates and Sandstones were deposited on an alluvial fan whereas thick mudstone sequences were laid down in a playa lake (MATTER 1987). Reduction spheres were found in all rock types, but are particularly abundant in the mudstones. Reduction spheres occur at present depths of 0 (outcrops) to 1'700 m (Riniken).

2.3 Triassic red beds

In the red beds of the Lower Triassic Bunter Sandstone, reduction spheres are much less common than in the Permian red beds. Reduction spheres with mineralized cores have only been found in the Bunter Sandstone of the Kaisten well.

3 INVESTIGATED SAMPLES AND ANALYTICAL METHODS

3.1 Sample provenience

Reduction spheres have been studied in samples from several wells (Weiach, Riniken, Kaisten, Zuzgen, Weierfeld, Wintersingen, Leuggern, Schafisheim) and two surface outcrops (Mumpf, Weitenau). Sample locations are marked on Figure 3. The most detailed investigations have been carried out on a 5 m-section of the Kaisten drillhole (Kai 226.65-231.25 m, in further text abbreviated as Kai 229, Fig. 2). From this interval, 5 average samples have been taken (representing 1 m each) for representative whole rock analyses. In addition to average bulk rock samples, representative samples of red zones, bleached haloes and core material have been obtained. Further on, detailed microscopic, microprobe- and U-series disequilibrium investigations (HOFMANN et al. 1987) have been done on samples from this section.

Comparative investigations have been carried out on reduction spheres from Jurassic/Cretaceous radiolarian cherts of the Warah formation (Oman). These samples have been kindly supplied by Tj. Peters and P. Steinmann.

3.2 Methods of investigation

Halo- and core size- and abundance have been determined from cut drillcores (10 cm wide) and from core photographs. The size-frequency distributions and core-abundance data (Fig. 4-8) are subject to geometric effects due to the determination from cut sections.

Most observations reported here rely on reflected- and transmitted light microscopy. Qualitative and quantitative microprobe analyses have been carried out using an ARL-SEMQ microprobe with wavelength- and energydispersive detector systems (operated at 15 kV, 20 nA). Analytical results have been corrected for atomic number, absorption and fluorescence (program EMMA). Bulk rock mineralogy has been determined by diffractometry using lithium fluoride as an internal standard. Clay minerals have been determined by diffractometry on oriented mounts of the <2μ fraction. Illite crystallinity data are given as half-width of the 001-peak in °2θ. Alpha-autoradiographs were made by exposing polished sections to Kodak LR 115 II films for several days to weeks and etching in KOH at 60°C (BASHAM & EASTERBROOK 1977). Chemical analyses were performed by standard XRF procedures using Li-tetraborate glass tablets for main- and pressed powder pills for trace analyses. U and Th were measured with a non-automatic XRF spectrometer following the procedure of JAMES (1977). DCP-analyses were carried out on acid digestions. FeO and B were determined by spectrophotometry, CO_2 and C_{org} by coulometry. Argon in roscoelites has been determined by mass spectrometry-isotope dilution (FLISCH

1982) and potassium by flame photometry. Instrumental neutron activation analyses (INAA) have been carried out by R. Alexander at the Scottish Universities Research and Reactor Centre (S.U.R.R.C.) in Glasgow.

4 PHENOMENOLOGY OF REDUCTION SPHERES

4.1 General

Three main optically and geochemically different zones can be distinguished in reduction spheres: I) Core, II) bleached halo and III) hematitic host rock. The size of reduction spheres ranges from less than 1 mm to 14 cm diameter in Northern Switzerland. The largest spheres reported are from South Devon with a diameter of up to 20 cm and a core mass reaching 9.5 kg (CARTER 1931). Cores of Northern Swiss reduction spheres range from 0.1 mm to 6 cm in diameter. Rarely, cores are structureless accumulations of finegrained ore minerals in a matrix of host rock minerals. More commonly, cores are composed of several concentric spherical layers differing in type and intensity of mineralization (Fig. 9). Even in large cores of 6 cm diameter, the innermost core nucleus may be only 1 mm in diameter and therefore accurately localizes the center of the structure. This indicates, that even large spheres developed from a point source of a reductant less than 1 mm in size. In some cases, an inner, intensely mineralized core can be distinguished from an outer, less mineralized core.

The transition from the mineralized core to the bleached halo is sharp. The bleached haloes differ from the enclosing host rock by the absence of the red coloration only. In some haloes, an inner, completely bleached zone is bordered by an outer, partly bleached zone. All transitions between the different zones are sharp even on a microscopic scale. In the hematitic host rock, no change of properties have been observed near reduction spheres. A more intense red pigmentation near spheres has been observed at some sites (Oman samples) indicating deposition of iron dissolved from spheres in the nearby red rock. Similar observations were made by MYAKURA & HAMPTON (1983).

4.2 Relation of reduction spheres to host rock heterogeneities and fractures

Reduction spheres in altered crystalline rocks and in red beds sometimes are concentrated on fracture surfaces (Sha 1968, Kai 297). In other cases, there is no association with such zones of enhanced permeability.

In the sediments, reduction spheres usually are randomly distributed. In some cases, they seem to be concentrated along coarser grained, more permeable sandstone layers and immediately above and below bleached sandstone horizons. This indicates that permeability may have played a role in reduction sphere genesis. However, reduction spheres also occur abundantly in thick layers of low-permeability clay.

Fractures postdating reduction sphere formation brought cores in contact with hematitic host rocks. Absence of bleaching in the hematitic rock in contact with the cores demonstrates that the reducing activity of the cores had ceased at that time. Similar observations have been reported by MEMPEL (1960) from Germany.

4.3 Size of reduction spheres and cores

Several authors have studied the size-relation between spheres and cores (PERUTZ 1940, EICHHOFF & REINECK 1952, HARRISON 1975). All these investigations showed that the relative size of the cores increases with increasing halo size. Similar measurements have been carried out for spheres from Weiach, Riniken and Kaisten (Fig. 4). No interpretable relation was found for the Weiach and Riniken spheres, probably due to the heterogeneity of the host rock (Riniken) and the low number of larger spheres (Weiach). The Kaisten spheres show the same trend as reported for the German and English spheres (e.g. HARRISON 1975): The larger the halo, the larger the relative size of cores. From the relation shown on Figure 4, halo: core volume-ratios (VR) of 300 for spheres 2 cm in diameter, VR = 64 for 4 cm diameter and VR = 27 for 6 cm diameter can be estimated. For the largest halo found (Mumpf), VR is about 13. On the other hand, the highest VR is greater than 1'000. For the largest spheres from South Devon (HARRISON 1975, Fig. 2) a VR of 6.5 can be estimated.

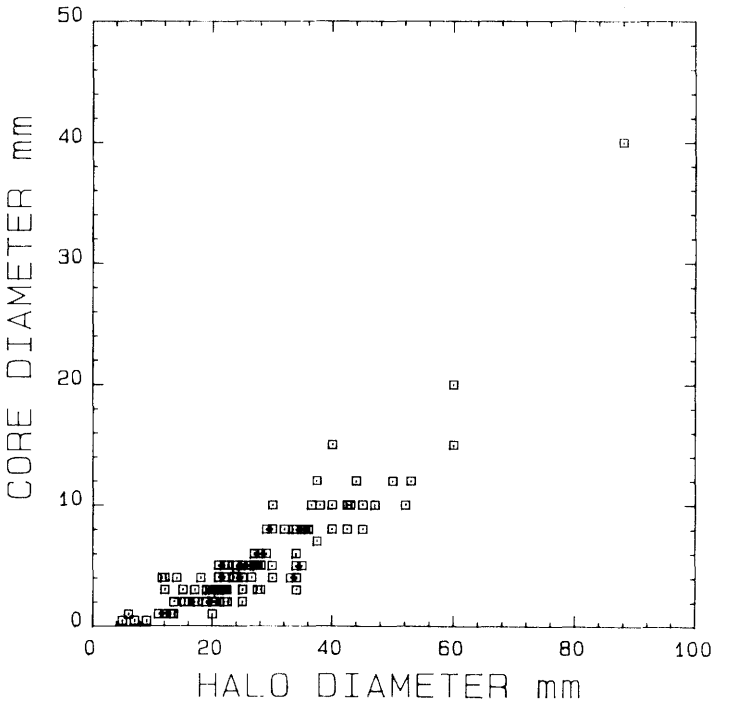

Fig. 4: Halo diameter versus core diameter of reduction spheres from the Kaisten well. For asymmetric spheres, the mean of the longest and the shortest axis is plotted.

4.4 Shape of reduction spheres

Most reduction spheres are not perfectly spherical but slightly oblate. This could be due to preferential diffusion parallel to the bedding or to compaction of the sediment after halo formation. Measurements of the ratios of the horizontal (b) to the vertical (a) axes of reduction spheres have been performed in Riniken and Weiach (MATTER et al. 1988). For Weiach, an average b:a of 1.35 has been obtained, in Riniken this ratio varies widely depending on host rock lithology and depth, b:a of mudstones in the upper part of the well are centered around 1.40. Own measurements on 108 cores from Kaisten yielded a mean b:a-ratio of 1.25 indicating the maximum compaction after halo formation was 20%.

4.5 Size distribution of reduction spheres and abundance of cores

The size distribution of spheres from Kaisten, Riniken and Weiach has been published by HOFMANN (1986). There is an exponential decrease in halo abundance with increasing size (Fig. 5). About 94% of all spheres are smaller than 1 cm. No bimodality has been observed for the total of all counted spheres. A detailed investigation in the Kaisten 229 m section has revealed that in this case a pronounced bimodality exists with 97.5% of all spheres smaller than 1 cm and a second maximum of abundance at a size of 25-30 mm. A similar bimodality has been observed by MYAKURA & HAMPTON (1984) in Warwickshire.

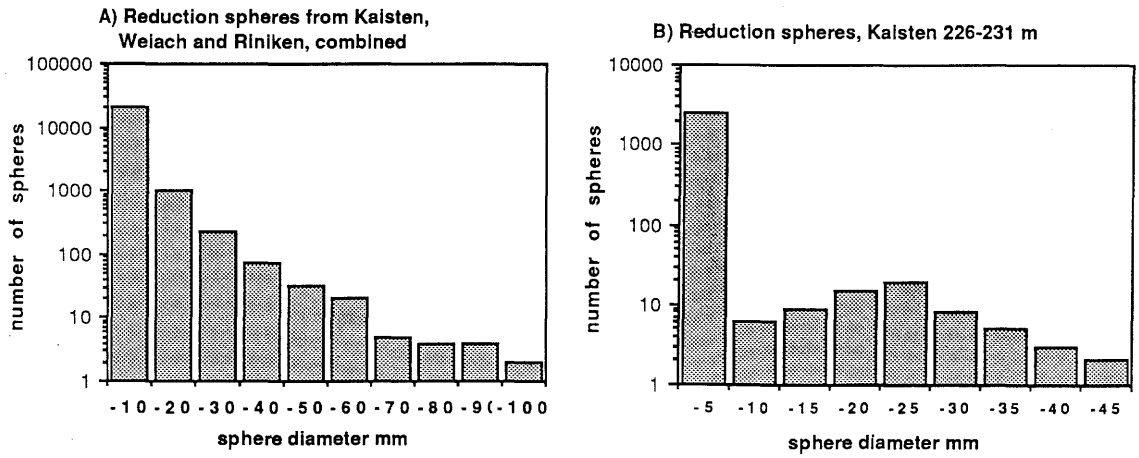

Fig. 5: Size-frequency-distribution of reduction spheres.

Generally, in Weiach, Riniken and Kaisten core abundance is a function of halo size (HOFMANN 1986). The larger the spheres are, the more frequently they do contain mineralized cores. The results obtained for Kaisten 229 m are somewhat different. Here, a larger proportion of small spheres are containing cores.

4.6 Abundance of reduction spheres, cores and irregular bleached zones

The abundance of reduction spheres and cores and the percentage of bleached (or originally drab) rock has been estimated in drillcore profiles of the Weiach, Riniken and Kaisten wells. The results are given for 10 m intervals in Figures 6, 7 and 8. There are some systematic trends. Bleached rock is most abundant in Weiach (21% above 1'170 m) but much less in Kaisten (7%) and Riniken (5%). Reduction halo- and core abundance seem to be negatively correlated with the abundance of reduced rock. This might indicate that reduction spheres and irregularly bleached zones are caused by the same type of reductant, but by a different process. The more common occurrence of bleached zones in Weiach might be due to the presence of underlying, organic-rich Autunian sediments which are missing in Kaisten and are at much greater depth in Riniken. Generally, reduction spheres and cores seem to be randomly distributed at small (dm) and large (hundreds of m) scale. For the Kaisten 229 m interval, the total abundance of spheres has been estimated as 6.2 vol.-%.

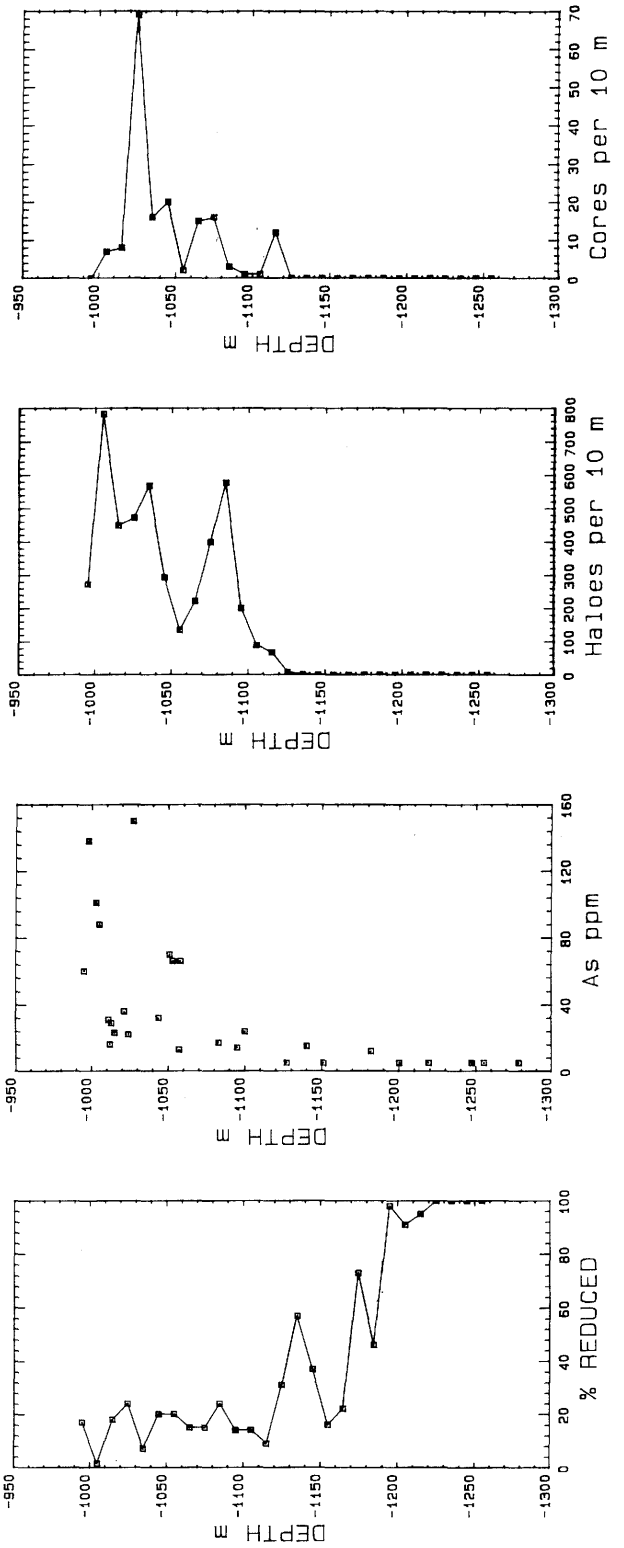

Fig. 6: Upper Permian red beds ("Oberrotliegendes", 991-1'170 m) of Weiach well: % reduced rock, As-concentration and abundance of haloes and cores versus depth. Data for 10 m-sections of 10 cm-wide cores = 1m². Depth = m below surface.

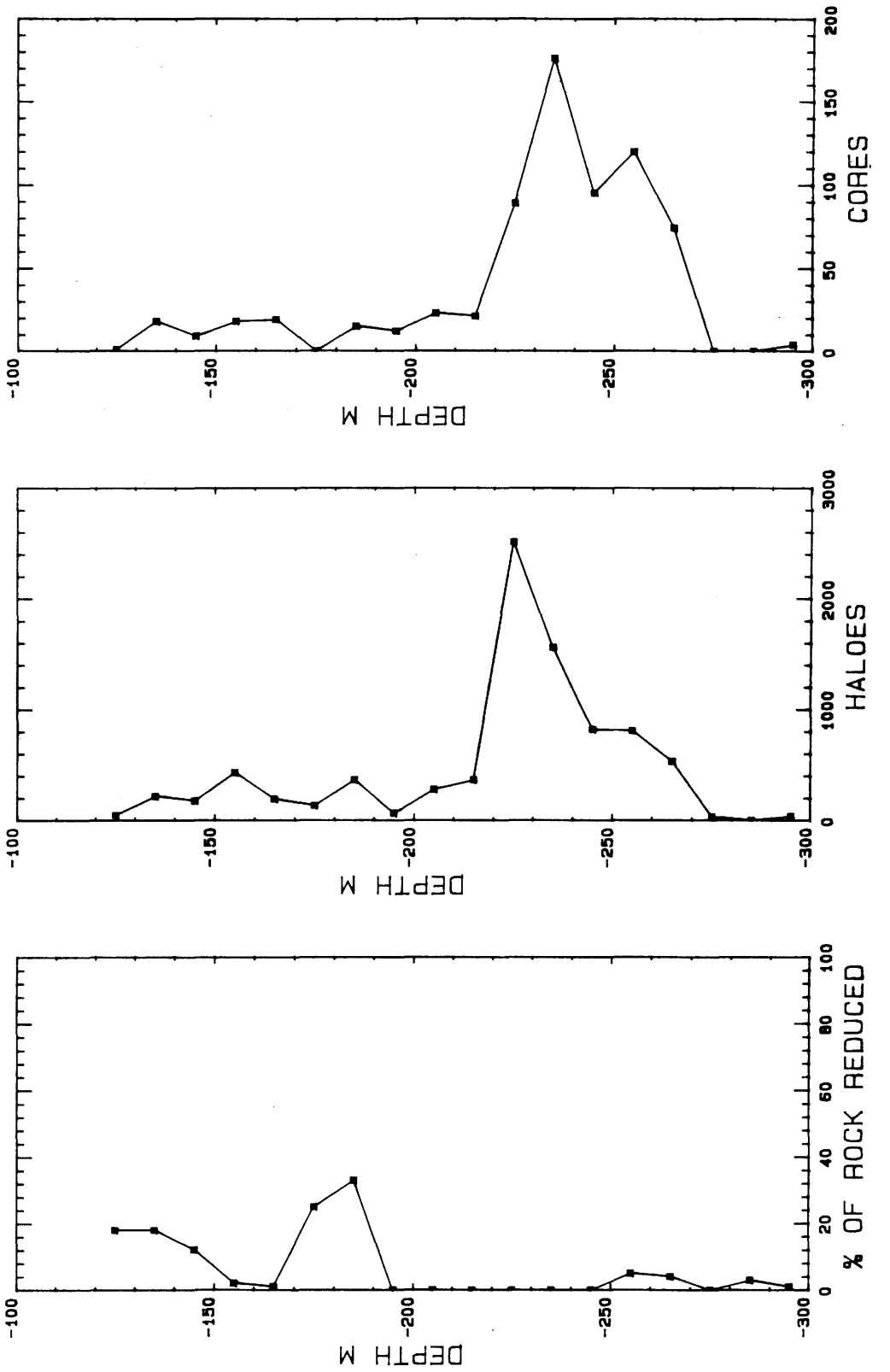

Fig. 7: Upper Permian red beds of Kaisten well: % reduced rock and abundance of haloes and cores versus depth. Data for 10 m-sections of 10 cm-wide cores = 1m² Depth = m below surface.

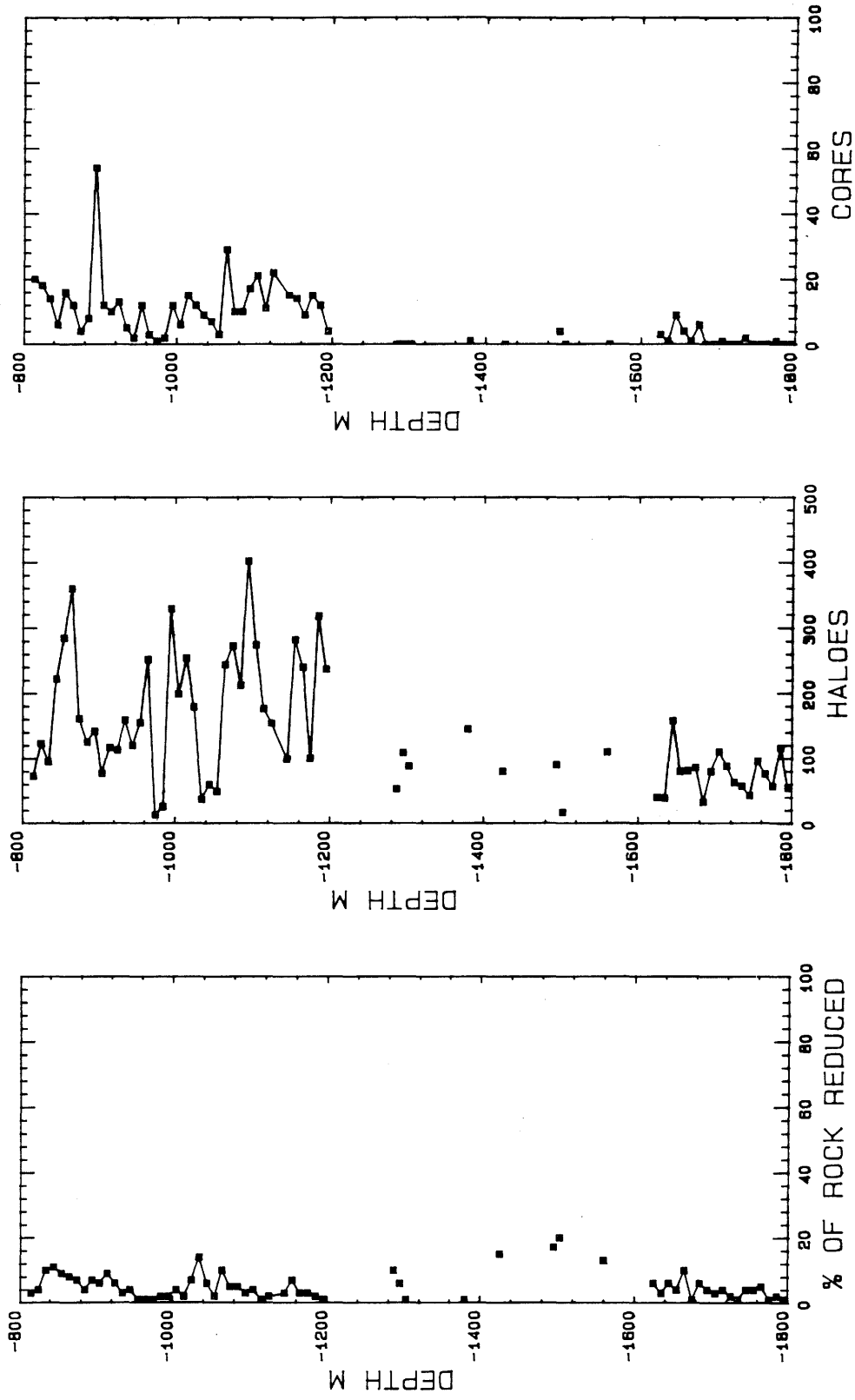

Fig. 8: Upper Permian red beds of Riniken well: % reduced rock and abundance of haloes and cores versus depth. Data for 10 m-sections of 10 cm-wide cores = 1m². Depth = m below surface.

5 MINERALOGY

5.1 Bulk rock and bleached zones

The bulk rock mineralogy of reduction halo containing rocks varies widely and the abundance of spheres seems not to be critically dependent on host rock mineralogy. The mineralogical composition of red beds from Riniken is given by MATTER et al. 1988 (enclosures 12, 13, 17). The main constituents of the Permian red beds are clay minerals (illite, chlorite, illite/smectite), quartz, K-spar, albite, calcite, dolomite and hematite. Minor constituents are anhydrite (occasional nodules) and heavy minerals. The mineralogy of the bulk rock of the Kaisten 229 m section is 21% quartz, 6% K-spar, 4% plagioclase, 4% calcite, 4% hematite, 1% dolomite and 60% clay minerals. The clay fraction < 2μm is made up of 95% illite and 5% chlorite.

No significant mineralogical difference has been found between bleached zones and the red host rock except for the absence of hematite in the bleached zones. Hematite occurs in two different forms in the red rock: I) Finegrained, submicroscopic hematite in the clay matrix and II) hematitized detrital grains, probably hematitized ferromagnesian silicates and pyrite. The latter grains are up to 20μm in diameter. Both types of hematite are completely dissolved in the bleached zones. The clay mineralogy of red and bleached rocks are identical, and there is no difference in illite crystallinity (0.71±0.06 in bleached haloes, 0.73±0.09 in red host rock). Detrital trace minerals include apatite, zircon, monazite, anatase, hematite-anatase intergrowths (altered ilmenite) and graphite. Placer-type enrichments of heavy minerals have been found at Kaisten (216.16). These heavy-mineral enrichments are not spatially associated with reduction spheres. Carbonates occur finely dispersed in the matrix of the rock, as cm-sized nodules of calcite and dolomite and as thin (< 1 mm) fracture linings of ankeritic dolomite and calcite postdating halo formation. It can be concluded that reduction halo formation is insensitive to host rock mineralogy and that no significant mineralogical change occurred in the bleached zones during the process of halo formation except for the dissolution of pigmentary iron oxides/hydroxides.

5.2 Mineralogy of the cores of reduction spheres

Reduction halo cores contain a very complex suite of ore minerals and some non-ore minerals absent in the host rock. Ore minerals form impregnations in the matrix of the host rock and replace rock-forming minerals. A list of authigenic minerals identified in the Northern Swiss reduction spheres are given in Table 1. At the different sites, significant differences have been found in the mineralogy of the

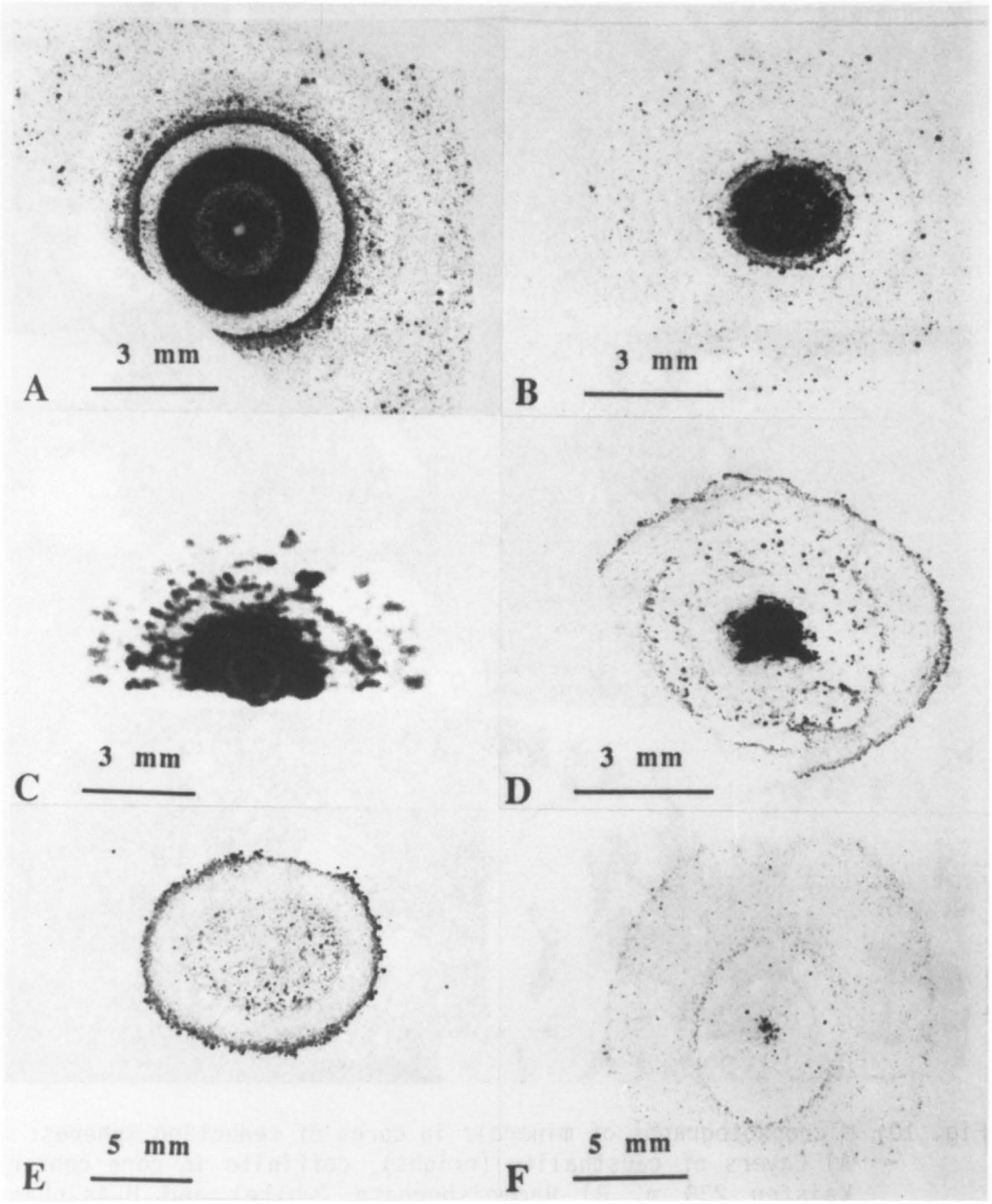

Fig. 9: Alpha-autoradiographs of reduction sphere cores showing distribution of alpha-particle-emitters (mostly U-phases). Exposure time varying from 1 to 3 weeks. A) Wef 257.6 m, B) Wef 245.0 m, C) Kai 230.0 m, D) Wef 125.6 m, E) Wef 170.0 m, F) Wef 166.4 m.

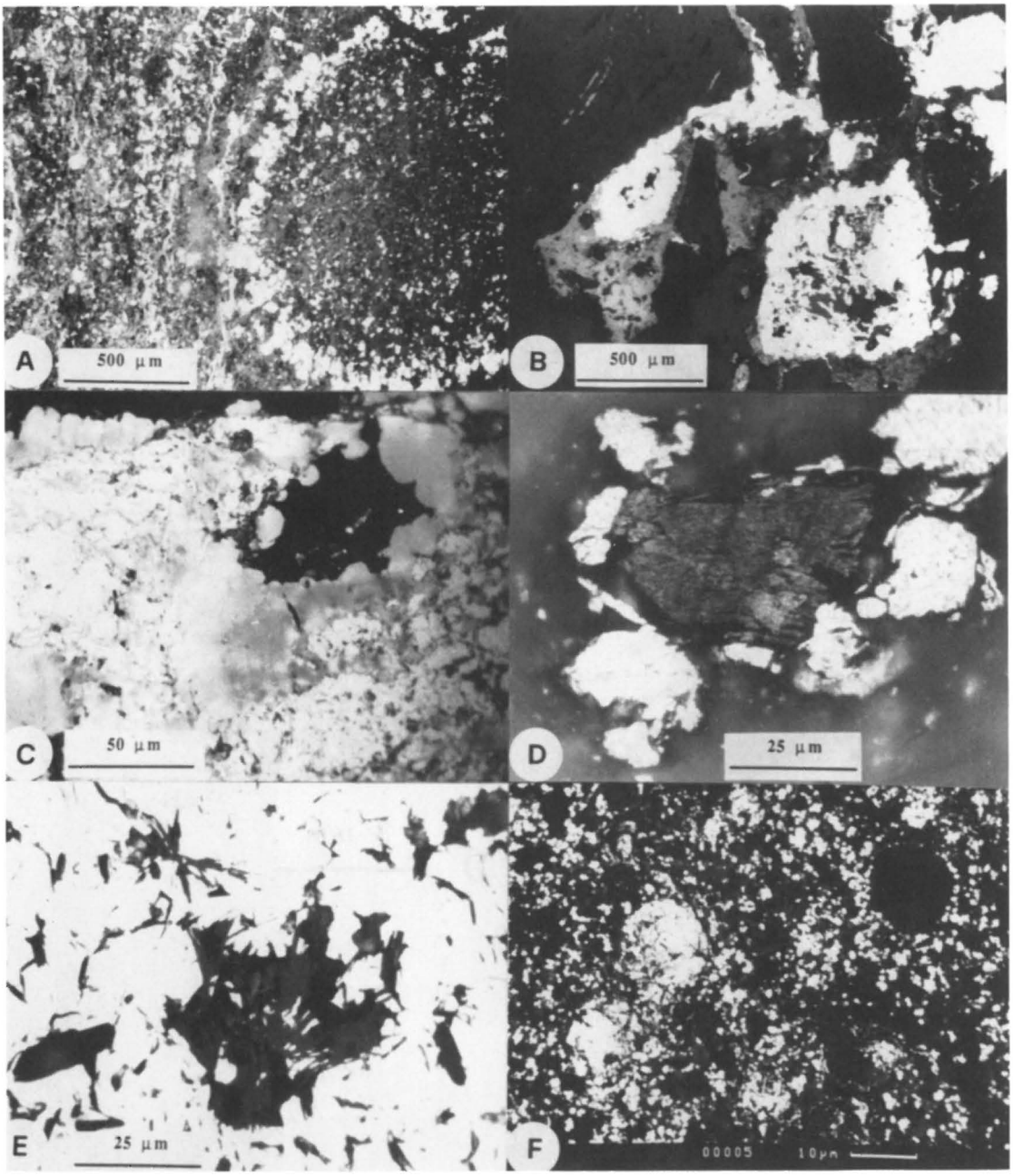

Fig. 10: Microphotographs of minerals in cores of reduction spheres:
A) Layers of causthalite (bright), coffinite in core center. Kaisten 230 m. B) Rammelsbergite (white) and U-As-phase (grey), Kaisten 129 m. C) Uraninite associated with anisotropic organic matter replacing detrital quartz grain (upper right corner). Weiach 1'076 m. D) Clausthalite (white) around detrital graphite flake, Zuzgen 227 m. E) Needles of U-As-phase (dark grey) in rammelsbergite. Kaisten 294 m.
F) Spherical structures of unknown (biogenic?) origin outlined by partly idiomorphic, REE-rich uraninite (bright). Backscattered electron image. Riniken 1'694 m.

cores. Also, changes of core mineralogy with depth have been noted in Riniken and Kaisten. Most ore minerals in reduction spheres are very finegrained, usually a few µm to a few 100µm, sometimes they form submicron-sized intergrowths with sheet silicates. The distribution of ore minerals in cores is well reflected in α-autoradiographs showing U-distribution (Fig. 9). Most determinations therefore rely on a combination of reflected light microscopy and microprobe analysis. The most common ore minerals or groups of ore mineral will be discussed individually.

Elements and intermetallic compounds: A broad suite of elements and intermetallic compounds occurs in reduction halo cores (Table 1,2). Native Cu and Cu-As-compounds only occur in the Weierfeld drillhole where they are quite common. The Weierfeld well is close to an occurrence of native copper in the Bunter sandstone at Kaiseraugst (WIENER 1975). Platinum-group minerals have been found in Kaisten (Pd-Sb), Weierfeld (Cu-Au-Pt-Se) and in Riniken (Pd-Bi). This latter mineral yields an atomic ratio of Pd:Bi close to 1 (Table 2). It is closest in composition to unnamed Pd(Bi,Pb) from Noril'sk (CABRI & TRAILL 1966).

Ni-Co-Arsenides: Among the most common ore mineral in reduction spheres are arsenides of nickel and cobalt. These minerals are common at all investigated sites except at Mumpf and in the lower parts of Riniken. The most common minerals are rammelsbergite $NiAs_2$, niccolite NiAs and chloanthite $NiAs_3$. Usually niccolite is the oldest mineral, it is overgrown and replaced by di- and triarsenides. Early arsenides are very finegrained and intimately intergrown with silicate minerals. Sometimes niccolite forms sponge-like masses. Microprobe-derived Ni-Co-Fe-relations are presented on Figure 11. In the reduction spheres, Ni-(Co)-rich arsenides are most abundant. Fe and S are only occasionally present in detectable amounts. The overall low Fe-content can be taken as an indication for the presence of very low ferrous iron concentrations in the porewater during the crystallization of the arsenides. In comparison, hydrothermal arsenides from veins in the Böttstein well contain more Fe (HOFMANN 1987). Palladium has been detected in one sample only of a rammelsbergite (0.05-0.14%). This is in contrast to similar parageneses in the Zechstein of Poland (KUCHA 1982, 1984), where arsenides are important Pd-carriers.

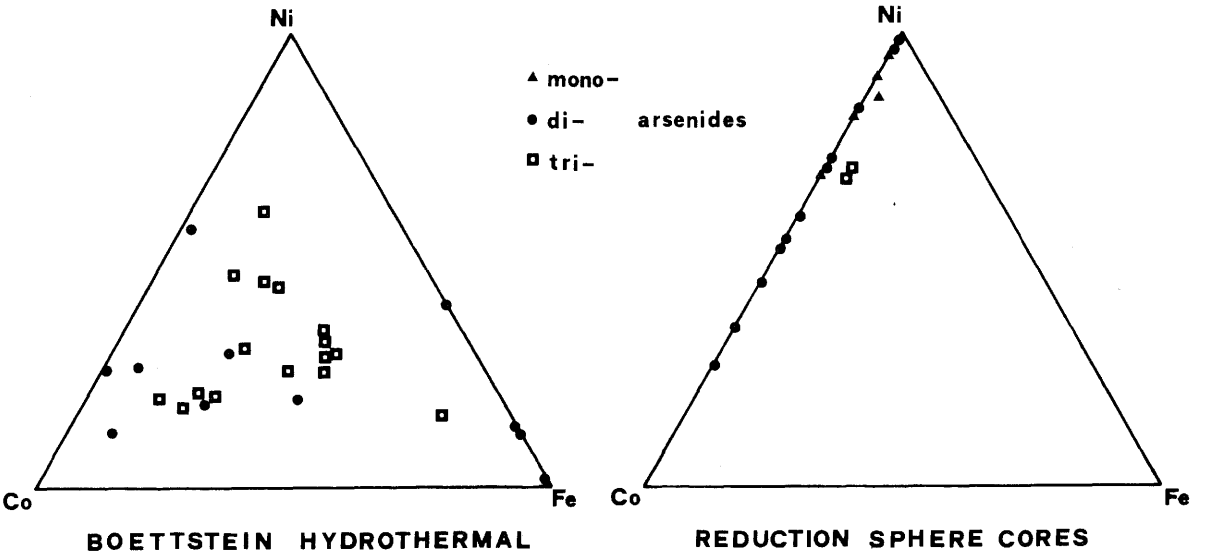

Fig. 11: Molar Ni-Co-Fe-relations (microprobe analyses) of arsenide minerals from hydrothermal veins of the Böttstein well and from reduction spheres in Permian red beds.

Sulfides: Although sulfides make up only a minor part of the ore minerals in most reduction sphere cores, they are quite widespread in small amounts. Most common are copper sulfides with compositions between Cu_2S and CuS. Both normal and "blaubleibender" covellite (probably corresponding to yarrowite and spionkopite) were observed.

Selenides, tellurides: Selenides are common in reduction spheres of all investigated sites except at Riniken. The most common selenides are clausthalite PbSe and bohdanowiczite $AgBiSe_2$. Berzelianite Cu_2Se, klockmannite CuSe, crookesite CuTlSe, guanajuatite Bi_2Se_3, naumannite Ag_2Se and a Cu-Au-Pt-Se-phase have been found only once each. Mineral formula derived from microprobe analyses are given on Table 2. The sulphur content of most selenides is very low indicating low activities of reduced sulphur species during selenide formation (TISCHENDORF & UNGETHÜM 1964).

Uraninite, brannerite and other U-phases: Uraninite is common in reduction spheres from all investigated sites except at Mumpf and in the lower part of Riniken. Uraninite is very finegrained (1 to 5µm, rarely up to 20µm) and forms small botryoids or replaces detrital silicates. Rarely, 1µm-size idiomorphic crystals have been observed. Representative microprobe analyses are given in Table 3. CaO, PbO, TiO_2 and SiO_2 are common minor elements and some samples show high concentrations of rare earth elements (Rin 1639: 6.56% REE oxides). All uraninites from reduction spheres show a particularly strong Sm-enrichment. Uraninites with similar contents of REE have been found in hydrothermal Co-Ni-Bi-Ag-U-mineralizations at Wittichen (Black Forest) and in the Böttstein well in Northern Switzerland. The high REE-content in the uraninites in reduction spheres indicates that REE-transport must have been coupled with a redox process, probably with ligand changes (REE-arsenate complexes ?). The lattice constant a_o has been determined for two samples and yielded values of 5.44 Å (Rin 893.1) and 5.38 Å (Wei 1089.8). These values are well within the range of Hercynian pitchblendes (CATHELINEAU et al. 1982).

Table 1: Authigenic minerals in the cores of reduction spheres

Occurrence in [1] Triassic red beds, [2] Permian red beds and [3] crystalline rocks

Elements, intermetallic compounds

silver Ag (+Au, Hg)[2], gold Au (+Ag, Hg)[2], copper Cu [2], auricupride (Au,Cu) [2], electrum (Au,Ag) [2], bismuth Bi [1,2], algodonite Cu_6As [2],
(Pd, Ag, Au, Pt)Bi [2], Pd-Sb [2], Cu-Ag-As [2], Cu-Ni-As [2], CuAs [2]

Arsenides

maucherite Ni_3As_2 [2], niccolite NiAs [2,3], rammelsbergite $NiAs_2$ [1,2,3], safflorite $CoAs_2$ [2,3], skutterudite (Ni, Co, Fe)As_3 [2,3]

Sulfides

chalcocite Cu_2S [2], digenite Cu_9S_5 [1,2,3], anilite Cu_7S4 [2], bornite Cu_5FeS_4 [1], stromeyerite CuAgS [2], sphalerite ZnS [3], chalcopyrite $CuFeS_2$ [1,2,3], tennantite $Cu_{10}Zn_2As_4S_{13}$ [1,2,3], tetrahedrite $Cu_{10}Zn_2Sb_4S_{13}$ [3], galenite PbS [2,3], covellite CuS [2], pyrite FeS_2 [3], cattierite $(Co,Fe)S_2$ [3]

Selenides, telluride

berzelianite Cu_2Se [2], crookesite CuTlSe [2], naumannite Ag_2Se [2], klockmannite CuSe [2], clausthalite PbSe [2], altaite PbTe [2], bohdanowiczite $AgBiSe_2$ [2], guanajuatite Bi_2Se_3 [2], Cu-Au-Pt-Se [2]

Oxides

uraninite UO_2 [2,3], brannerite UTi_2O_6 [2], uraniferous leucoxene $nTiO_2.UO_2$ [2,3], montroseite VOOH [2], cuprite Cu_2O [2], U-As-oxide [2,3],

Phosphate

apatite $Ca_5[F|(PO4)3]$ [2]

Silicates

roscoelite $KV_2(OH)_2AlSi_3O_{10}$ [2,3] , coffinite $USiO_4$ [1,2,3]

Table 2: Mineral formula (at %) derived from microprobe analyses

Elements	
$Au_{94.8}Ag_{2.3}Cu_{0.8}Bi_{0.5}Hg_{1.6}$	native gold, Wef 258 m
$Au_{89.4}Ag_{8.8}Cu_{0.3}Bi_{0.5}Hg_{1.0}$	native gold, Kai 208 m
$Ag_{64.6}Au_{35.2}Bi_{0.2}$	electrum, Kai 208 m
$Ag_{97.8}Au_{0.7}Cu_{0.1}Hg_{1.4}$	native silver, Kai 208 m
$Ag_{97.9}Hg_{2.1}$	native silver, Kai 218 m
$Cu_{99.83}Ag_{0.02}As_{0.15}$	native copper, Wef 126 m
$Cu_{85.47}Ag_{0.02}As_{14.49}Bi_{0.01}Hg_{0.01}$	±algodonite, Wef 126 m
$Pd_{37.14}Cu_{6.57}Ag_{2.55}Pt_{0.60}Au_{0.18}Bi_{52.62}As_{0.29}Sb_{0.05}$	±PdBi, Rin 1639 m
$Cu_{43.5}Au_{16.01}Pt_{7.65}Ag_{1.71}Se_{31.22}$	unknown phase, Wef 258 m
Selenides, telluride	
$Cu_{63.38}Ag_{0.15}Se_{36.28}S_{0.19}$	berzelianite, Wef 258 m
$Cu_{56.91}Ag_{0.06}Tl_{8.36}Se_{34.52}S_{0.15}$	crookesite, Wef 258 m
$Pb_{49.91}Ag_{0.69}Se_{49.27}Te_{0.13}$	clausthalite, Kai 208 m
$Pb_{50.53}Ag_{0.60}Te_{47.33}Se_{1.54}$	altaite, Kai 208 m
$Ag_{23.18}Bi_{25.73}Se_{50.34}S_{0.40}Te_{0.35}$	bohdanowiczite, Mumpf

Brannerite and coffinite are less common than uraninite. Brannerite occurs in crystals up to 15µ in sample Rin 1639 (analysis on Table 3). These crystals clearly postdate early, finegrained uraninite and have a lower Pb/U-ratio. There are gradual changes from brannerites with U:Ti = 1:1 to slightly uraniferous leucoxenes. The higher the U content, the darker the color of leucoxene. Coffinite is quite common but usually very finegrained. EDS spectra of coffinite indicate the presence of variable but important amounts of P in addition to U and Si. In Kaisten (129 m, 294 m, 351 m) a very As-rich, needle-forming black U phase has been found. The optical properties of this mineral are very close to those of coffinite. This As phase has a very low Pb content, that could either be due to low Pb-retentivity or low age.

Apatite has been found in two reduction spheres in Riniken. Rin 1295.32 is a core composed of finegrained apatite (collophane). This apatite replaces detrital minerals and is clearly authigenic. The x-ray pattern (Guinier camera) indicates the presence of F-apatite. In sample Rin 1639.46, apatite is intimately intergrown with uraninite. Since chemical analyses do not show a general P-enrichment in sphere cores, the occurrence of apatite must be sporadic. Phosphate-enrichment cannot be directly explained by a redox process.

Roscoelite (vanadian mica) is the most common authigenic mineral in reduction spheres. Most of the dark coloration of sphere cores is due to the presence of this mineral. Roscoelite has been found abundantly at all sites except in the lower part of the Kaisten well (below 231 m). In the lower part of the Riniken well, roscoelite is the only ore mineral present in reduction spheres and irregularly bleached zones. In the irregularly bleached zones (Rin 1067, Rin 1739) pure roscoelite aggregates 1-2 cm in diameter have been found. The crystallinity of the roscoelites is better than that of associated illites (3 roscoelites: 0.40±0.11, 10 illites: 0.72±0.07). SEM images show that individual roscoelite crystals are up to 30µm in size with an average grain size of 5-10µm. Microprobe analyses of 6 roscoelites from Northern Swiss reduction spheres are presented in Table 4 and compared with roscoelite in a reduction sphere from East Greenland and a hydrothermal roscoelite from the Black Forest. The pure roscoelites are quite rich in V_2O_3 (24.4-26.0%) compared with other published roscoelite analyses (9.9-12.1%, SCHADE et al. 1986; 14.3-23.6%, JOHAN & POVONDRA 1987). 64 to 79% of the octahedral positions are occupied by V. Sample Sha 1968 (reduction sphere from the crystalline basement) differs from the other roscoelites by a higher V- and a lower Al-content. In this mineral, V must replace some tetrahedral Al in addition to octahedral Al. The B-content of one sample (Rin 1068) is 40 ppm indicating that no B-enrichment has occurred in this mineral relative to the host rock (171 ppm B). The V_2O_3-content of pure cores is 7.3 to 7.7% (Table 8), indicating the presence of about 30% roscoelite in highly mineralized cores.

Table 3: Microprobe analyses of uranium minerals from cores of reduction spheres (mean of n analyses)

Sample Nr.	Wei1076	Rin1639P	Rin1639B	Wef804	Kai230	Kai129	Kai294	Kai351
n	8	6	6	5	5	6	7	8
Weight %								
UO_2	90.30	86.73	45.92	91.94	60.88	81.54	77.88	72.68
TiO_2	0.29	0.9	38.48	0.45	0.32	1.20	1.93	1.66
PbO	1.68	1.58	0.59	1.75	1.09	0.00	0.07	0.00
CaO	2.56	1.53	2.28	2.01	1.02	2.04	1.20	1.45
SiO_2	0.60	1.32	1.51	0.57	9.04	1.39	2.13	2.00
ThO_2	0.00	0.09	0.00	0.02	0.00	0.00	0.04	0.55
As_2O_3	0.00	0.04	0.00	0.00	2.98	6.38	6.30	9.85
Y_2O_3	0.46	1.78	1.21	0.94	2.73	0.27	0.04	0.22
La_2O_3	0.00	0.18	0.00	0.00	n.a.	n.a.	n.a.	0.00
Ce_2O_3	0.00	0.80	0.00	0.29	n.a.	n.a.	n.a.	0.00
Nd_2O_3	0.28	1.96	1.69	0.00	n.a.	n.a.	n.a.	0.05
Sm_2O_3	0.25	1.29	0.96	0.00	n.a.	n.a.	n.a.	0.15
EuO	0.05	0.39	0.18	0.00	n.a.	n.a.	n.a.	0.00
Gd_2O_3	0.27	0.68	0.13	0.79	0.00	0.04	0.03	0.13
Dy_2O_3	0.29	0.88	0.56	0.00	n.a.	n.a.	n.a.	0.20
Er_2O_3	0.00	0.38	0.00	0.00	n.a.	n.a.	n.a.	0.00
Total	97.03	100.53	93.51	98.76	78.06	92.86	89.62	88.94

Wei 1076: Pitchblende associated with organic matter. Weiach 1076 m
Rin1639P: Pitchblende, Riniken 1639 m
Rin1639B: Brannerite, Riniken 1639 m
Wef 804: Pitchblende, Weierfeld well

Kai 230: Coffinite, Kaisten 230.00 m
Kai 129: U-As-Phase, black, Kaisten 129 m
Kai 294: U-As-Phase, black needles. Kaisten 294 m
Kai 351: U-As-Phase, black needles, reduction zone in top of crystalline. Kaisten 351 m

Table 4: Microprobe analyses of roscoelites

Sample Nr.	Rin 1769/1	Rin 1769/2	Rin 1068	Rin 1032/1	Rin 1032/2	Sha 1968	Wut	GR 22
n	6	3	4	4	4	2	4	2
Weight %								
SiO_2	46.19	44.03	39.14	45.19	44.57	41.37	43.62	42.80
TiO_2	0.03	0.16	0.00	0.04	0.52	0.00	0.00	0.00
Al_2O_3	17.05	17.15	11.43	15.58	19.21	4.50	11.74	11.63
V_2O_3	25.96	24.61	26.00	24.39	13.82	36.48	27.60	29.30
Cr_2O_3	0.37	0.36	0.33	0.37	0.23	0.50	0.39	0.43
FeO	0.59	0.82	0.13	0.78	0.83	0.00	0.14	0.00
MgO	1.83	1.97	1.31	1.66	1.76	3.25	2.64	2.92
CaO	0.34	0.16	0.25	0.25	0.08	0.18	0.53	0.25
K_2O	8.30	8.31	7.74	8.84	8.37	8.16	7.35	7.17
Total	100.66	97.57	86.33	97.10	89.39	94.44	94.01	94.50
Mineral formulas: Atoms per 22 oxygens								
Si	6.172	6.141	6.271	6.341	6.558	6.376	6.357	6.232
Ti	0.003	0.017	0.000	0.004	0.058	0.000	0.000	0.000
$Al^{(IV)}$	1.828	1.859	1.729	1.659	1.442	0.817	1.643	1.768
$Al^{(VI)}$	0.857	0.960	0.429	0.918	1.889	-	0.373	0.228
V	2.781	2.752	3.340	2.744	1.630	4.508	3.225	3.420
Cr	0.039	0.040	0.063	0.041	0.027	0.061	0.045	0.050
Fe	0.066	0.096	0.017	0.092	0.102	0.000	0.017	0.000
Mg	0.365	0.410	0.313	0.347	0.386	0.747	0.573	0.634
Ca	0.049	0.024	0.043	0.038	0.013	0.030	0.083	0.039
K	1.415	1.479	1.582	1.582	1.571	1.604	1.366	1.332

Rin: Riniken samples, /1 : analyzed in polished section, /2 : K/Ar-separates analyzed on graphite tablets
Sha: Schafisheim sample (reduction sphere in granite breccia)
Wut: Hydrothermal roscoelite from quartz vein, upper Wutach valley, Black Forest
GR 22 Roscoelite in reduction sphere, Triassic red beds, Pingo Dal, Jameson Land, East Greenland

Carbonates in reduction spheres: Carbonates intimately associated with ore minerals are calcite and dolomite. Microprobe analyses show that both minerals are free of iron (< 0.01%) but do contain 0.2 to 5.7 mol% $MnCO_3$. This indicates low ferrous iron concentrations during carbonate crystallization. Small veinlets of dolomite postdating the formation of reduction spheres are iron-bearing (2.6 mol% $FeCO_3$) indicating the predominance of more reducing conditions after sphere formation.

Organic matter: The presence of organic matter intimately intergrown with ore minerals in reduction spheres has been ascertained in sphere cores from Weiach. The organic matter is often associated with U-minerals and shows the typical features of radiation-damaged kerogen: High reflectivity and strong anisotropy (Fig. 10). For organic matter from sample Weiach 1076.64, the following properties determined: Reflectivity in air (530 nm): 12.0±0.9% (n = 13, range 10.3-13.2), Vickers hardness 350-550. Microprobe analyses showed no detectable U in the organic matter a few microns away from uraninite. In the EDS-spectrum, small peaks of Cl, Si and S were visible. The organic matter is replacing detrital quartz grains.

Organic matter is present in many occurrences of reduction spheres, sometimes as main constituent (PIERCE et al. 1964, CURIALE et al. 1983, PARNELL 1985, PARNELL & EAKIN 1987), sometimes as trace only (EICHHOFF & REINECK 1952, HARTMANN 1963, HARRISON 1975). Absence of organic matter in reduction spheres has been reported by VAN DE POLL & SUTHERLAND (1976). The organic matter-U-association in reduction spheres in many respects resembles "thucholite" and "carburan" described from various uranium deposits (ELLSWORTH 1928, GRIP & ÖDMANN 1944, SCHIDLOWSKI 1981, LEVENTHAL et al. 1987).

It is unclear whether the observed organic matter is a residue of the organic matter that was involved in sphere formation or whether it is a secondary accumulation due to the presence of radioactive uraninite causing the polymerization of mobile organics.

Graphite occurs as detrital flakes in the Permian red beds of Northern Switzerland. Graphite flakes observed in reduction sphere cores are often enveloped by ore minerals (Fig. 10). This might be taken as an indication for redox reactions between the porewater and graphite. Similar features have been observed in dolomite nodules in Permian red beds of Czechoslovakia by JOHAN & POVONDRA (1987, Fig. 2d). To check for a possible involvement of detrital graphite in reduction sphere formation, graphite flake abundance was estimated by counting of flakes in polished thin sections (oil immersion, reflected light). No difference in graphite abundance in cores, bleached haloes and red host rock was found. Therefore, it is concluded that detrital graphite has not played an important role in reduction sphere formation. The graphite content has been estimated as 60±20 ppm by volume (Kai

230.0 m). Textural reasons exclude an authigenic origin of this graphite as proposed for graphite in the Zechstein copper deposits of Poland (KUCHA 1988).

5.3 Mineralogical comparison with other described occurrences of reduction spheres and with ore deposits

Mineralogical descriptions of reduction sphere cores from localities other than N Switzerland are given by HARRISON (1975, S Devon), PIERCE et al. (1964, N Texas), CURIALE et al. (1983, SW Oklahoma), VAN DE POLL & SUTHERLAND (1976, New Brunswick) and FESSER (1971, Helgoland, N Germany). The mineralogy of the reduction spheres of S Devon is very similar to those from Northern Switzerland. HARRISON (1975) describes roscoelite, coffinite, copper, silver, safflorite and others. Investigations by the author showed that montroseite is also present. VAN DE POLL & SUTHERLAND (1976) describe roscoelite, cuprite, copper, and schucherite (silver-amalgam). On Helgoland, reduction sphere cores contain native Cu, cuprite, chalcopyrite, domeykite (FESSER 1971) and roscoelite (author's investigation, 1987). Roscoelite is a common mineral in reduction spheres from E Greenland (HOFMANN 1986), from Oman (this paper) and in dolomite nodules from Czechoslovakia (JOHAN & POVONDRA 1987). The organic-rich cores of N Texas and SW Oklahoma seem to contain less ore minerals. Clausthalite, uraninite, skutterudite and pyrite have been reported (PIERCE et al. 1964, CURIALE et al. 1983).

It can be concluded that the cores of reduction spheres usually contain roscoelite and a broad suite of ore minerals of U, Cu, Ni, Co, As etc. Sulfides are less abundant, usually sulfides of Cu are present only. The mineralogy of the Northern Swiss reduction spheres is so far the most diverse described, but this is probably due to the relatively large amount of samples available for investigation. There are strong similarities with parageneses described by KUCHA (1982, 1984) from the Zechstein copper deposits in Poland, where a similar association of Ni-Co-arsenides, U-minerals, selenides, kerogen, phosphate and precious metals (Ag, Au, Pd, Pt) has been described. Close paragenetic similarities also exist with unconformity-type U-deposits in the Athabasca basin (HOEVE & SIBBALD 1978) and with roll-type- and tabular U-V-deposits of the Colorado Plateau (WEEKS et al. 1959) where roscoelite is common as well (FOSTER 1959).

6 POROSITY

The porosity of host rocks, spheres and core material was measured for the Kaisten 229 m section and for some additional pairs of samples of spheres and red host rock. Porosity was determined as difference of bulk- and grain density. Bulk rock densities were determined by immersion in mercury, grain density by a pyknometric method. 11 bulk samples of red host rock (clay) averaged 11.3±0.8 vol.-% total porosity. In sample Kai 218.48, sphere (13.1%) and bulk rock (13.9%) had a somewhat higher porosity. Samples of a very large sphere with core (Zuzgen 227.25) yielded the following results for different zones: Core 5.8 %, bleached zone 8.5%, red host rock 9.9%. The overall lower porosity in this sample is due to a higher content of quartz grains.

Selected samples were investigated by mercury porosimetry. 4 samples from Kaisten (218.48 and 230.00 m, bleached and red zones each) showed that 79-89% of all pores have entrance radii smaller than 63 Å (limitation of apparatus used). In the different zones of Zuzgen 227.25 m, 27-87% of pores are smaller than 63 Å. No significant difference was found in porosity between bleached zones and enclosing host rock.

Two samples of core material showed reduced total porosity and a bimodal poresize distribution with a first maximum at 0.1µm and a second at poresizes smaller than 100 Å similar to the unmineralized samples. Since the larger pores were found only in the cores, they must be related with mineralization and possibly are due to redissolved ore phases. The lower total porosity in mineralized samples is due to cementation of porespace by ore minerals.

7 GEOCHEMISTRY OF REDUCTION SPHERES AND ENCLOSING ROCKS

Geochemical analyses of different zones in reduction spheres (cores, bleached haloes, hematitic host rock, bulk rock) were carried out on samples from three different sites. The most detailed work was done on the Kaisten 229 m section, where samples each of bulk rock, red host rock, bleached haloes, and cores have were analyzed for main- and trace elements by XRF and INAA. From Mumpf, one representative sample of red zone, reduced zone and cores was analyzed. From the Riniken well, the three zones of two spheres were analyzed for Fe, Mn, Ni, Co and Cu by DCP spectrometry. Three average bulk samples of organic-rich Autunian sediments underlying the red-bed sequence in Weiach were analyzed as well. The data are presented on Tables 5, 6 and 7.

Analysis of individual cores, haloes and host rocks also was attempted by microprobe analysis of polished thin sections (Tables 8,9). The probe was operated in the scanning mode. The results obtained for single spheres are in reasonable agreement with XRF analyses of composite sphere zones.

7.1 Results

As can be expected from the highly variable mineralogy of sphere cores and the variability of the host rocks, the results obtained on samples from different sites are highly variable. Among the main elements, only ferric iron shows systematic variations. In the bleached zones and in the cores, the ferric (and total) iron content is much lower than in the red host rock. This shows that hematite has been dissolved and carried away (as ferrous iron or possibly as organic ferric iron complex). The difference in ferric iron content between bleached zones and red host rock correspond to a hematite content of 3.8% at Kaisten, 2.3% at Mumpf and 3.0/1.0% at Riniken. The observation of red bed bleaching being due to hematite dissolution and removal of Fe confirms similar results of EICHHOFF & REINECK (1952), HARTMANN (1963) and DURRANCE et al. (1978). Among the trace elements, only V, U, Cr, Cu and Se are enriched in Mumpf. In Kaisten, however, V, U, Cr, Cu, Ce, Nd, Pb, Ni, Co, Zn, As and Se are enriched. The analyses of Ni, Co, Cu for the Riniken samples indicate a similar type of enrichment as in Kaisten. The available information indicates that Ti, Zr, Hf, Ta and Th were immobile during reduction sphere formation.

For the Kaisten 229 m section, mass-balance calculations have been performed using the following volume fractions for the different zones: red rock 0.938, bleached zones 0.0615, cores 0.0005 (estimated by point-counting from core photographs). Assuming a homogeneous trace element distribution before sphere formation commenced, the fraction of an element mobilized during reduction sphere formation can be deduced in two ways:

Table 5: Chemical analyses (XRF) of bulk rocks, red host rocks, bleached haloes and cores

Sample Nr.	Weiach Autunian (drab beds)	Kaisten 230 bulk red bed with spots	Kaisten 230 host red bed	Kaisten 230 bleached haloes	Kaisten 230 cores	Mumpf host red bed	Mumpf bleached haloes	Mumpf cores
n	3	10	5	5	1	1	1	1
Weight %								
SiO_2	55.82	56.37	57.11	59.27	57.70	66.11	68.21	68.06
TiO_2	1.04	0.85	0.87	0.89	0.82	0.47	0.31	0.29
Al_2O_3	20.54	17.65	17.56	17.71	16.92	12.65	11.92	12.07
Fe_2O_3	1.54	5.91	6.27	2.44	0.53	3.24	0.90	0.78
FeO	4.42	0.76	0.76	0.80	1.74	n.a.	n.a.	n.a.
MnO	0.04	0.09	0.08	0.08	0.07	0.05	0.05	0.04
MgO	2.26	2.55	2.55	2.57	1.64	2.76	2.58	2.23
CaO	0.68	2.79	2.02	2.77	2.54	2.38	2.82	2.32
Na_2O	1.58	0.47	0.51	0.59	0.52	0.37	0.88	1.25
K_2O	3.88	6.02	6.12	5.98	6.00	4.56	4.54	4.87
P_2O_5	0.31	0.22	0.23	0.23	0.20	0.15	0.14	0.12
H_2O+	4.43	3.74	3.39	3.74	3.13	3.38	2.21	2.11
CO_2	0.50	2.10	2.08	2.11	1.76	3.34	3.56	2.79
C_{org}	1.24	0.00	0.00	0.00	0.00	n.a.	n.a.	n.a.
Traces	0.21	0.22	0.21	0.24	2.96	0.16	0.15	1.00
Total	98.49	99.74	99.76	99.42	96.53	99.62	98.27	97.93
ppm								
Ba	512	478	505	485	486	603	671	677
Rb	260	383	363	379	307	234	206	229
Sr	121	176	171	179	105	152	167	135
Pb	35	52	51	29	601	15	<10	<10
Th	29.8	17.5	18.0	15.2	10	<10	12	18
U	9.8	7.9	6.5	12.9	1614	<2	2.5	21.3
Nb	23	18	17	17	6	7	<5	<5
La	101	88	82	76	68	43	23	35
Ce	112	82	75	82	1279	63	30	29
Nd	48	23	19	20	99	18	18	18
Y	39	37	36	36	16	20	18	16
Zr	234	209	220	216	137	178	185	175
V	155	153	143	216	10420	78	77	8470
Cr	107	93	90	88	156	34	19	52
Ni	53	57	50	71	2520	25	15	14
Co	24	22	21	17	379	10	2	<2
Cu	33	9	9	15	142	8	6	19
Zn	84	109	105	108	146	55	37	63
Ga	32	24	24	25	21	17	13	13
Sc	26	24	23	24	18	11	6	6
As	<5	102	74	292	10800	49	34	24
B	58	171	n.a.	n.a.	n.a.	n.a.	n.a.	n.a.
Se	<1	<1	<1	<1	85	n.a.	n.a.	n.a.

Table 6: INAA analyses, Kaisten

	Sc	Co	Ta	Ce	Nd	Eu	Lu	Hf
229.83bulk	26.5	17.5	1.9	n.d.	n.d.	1.8	n.d.	11.5
229.83red	26.1	14.0	2.1	n.d.	n.d.	1.9	2.9	10.0
229.83halo	24.4	16.9	2.2	n.d.	n.d.	1.6	n.d.	7.0
230.78bulk	23.5	18.1	2.0	n.d.	n.d.	1.4	n.d.	9.4
230.78red	24.6	17.5	1.5	n.d.	n.d.	1.5	2.3	10.0
230.78halo	23.7	26.2	2.3	n.d.	n.d.	1.7	2.8	10.1
Core composite	22.3	832	n.d.	1200	960	2.0	69	8.8

Table 7: Concentrations of some elements in different zones of two reduction spheres from Riniken (DCP)

	Fe%	Mn	Ni	Co	Cu
Rin 826.6					
Core (0.55g)	1.1	280	33000	23000	950
Halo (8.1g)	2.0	480	130	45	18
Host rock	5.0	430	60	28	14
Rin 933.4					
Core (0.5g)	0.13	360	83	96	390
Halo (226g)	0.50	270	22	18	9
Host rock	1.50	650	26	15	9

Table 8: Microprobe analyses of different zones in individual reduction spheres

Sample Nr	Kai 230 inner core	Kai 230 outer core	Kai 230 inner halo	Kai 230 outer halo	Kai 230 host near halo	Kai 230 host rock
n	5	5	5	5	5	5
Weight %						
SiO_2	53.01	55.59	53.23	55.65	53.29	50.10
TiO_2	0.89	0.66	0.78	0.79	0.83	0.99
Al_2O_3	17.09	16.96	19.21	17.49	18.60	18.72
Fe_2O_3 (tot)	2.60	2.63	4.05	3.60	6.98	7.37
V_2O_3	7.35	2.59	0.00	0.00	0.00	0.00
Cr_2O_3	0.11	0.07	0.00	0.00	0.00	0.00
MnO	<0.03	<0.03	0.05	0.08	0.07	0.07
MgO	2.26	2.07	2.51	2.06	2.32	2.31
CaO	0.43	1.66	1.06	1.90	0.81	0.77
Na_2O	0.30	0.38	0.28	0.26	0.32	0.23
K_2O	7.45	6.98	7.60	7.35	7.54	7.77
Total	91.46	89.62	88.77	89.18	90.76	88.33

Sample Nr	Kai 231 inner core	Kai 231 outer core	Kai 231 inner halo	Kai 231 outer halo	Kai 231 host near halo	Kai 231 host rock
n	5	5	5	5	5	5
Weight %						
SiO_2	54.01	57.87	53.68	54.98	55.61	52.04
TiO_2	0.95	0.65	0.55	1.14	0.80	0.50
Al_2O_3	16.86	14.75	17.78	18.29	15.49	15.62
Fe_2O_3 (tot)	2.42	2.45	4.01	4.69	6.69	5.29
V_2O_3	7.72	1.71	0.00	0.00	0.00	0.00
Cr_2O_3	0.19	0.05	0.00	0.00	0.00	0.00
MnO	<0.03	0.03	0.14	0.08	0.11	0.13
MgO	2.29	1.90	2.21	2.48	2.24	1.78
CaO	1.27	3.98	4.97	1.88	3.74	5.93
Na_2O	0.49	0.37	0.40	0.39	0.42	1.20
K_2O	7.20	6.14	6.91	6.88	5.63	5.38
Total	93.43	89.90	90.65	90.81	90.73	87.87

Table 9: Microprobe analyses of different zones in a reduction sphere from radiolarian cherts of the Warah formation, Oman

Sample Nr	OM 106 core	OM106 halo	OM106 host near halo	OM106 host rock
n	5	5	5	5
Weight %				
SiO_2	79.15	87.88	85.81	85.72
TiO_2	0.14	0.06	0.30	0.11
Al_2O_3	4.99	1.69	2.59	2.89
Fe_2O_3 (tot)	0.40	0.36	1.48	1.17
V_2O_3	6.06	0.08	0.02	0.00
Cr_2O_3	0.13	0.00	0.00	0.00
MnO	0.06	0.00	0.06	0.07
MgO	1.46	0.25	0.00	0.00
CaO	0.50	0.23	0.34	0.35
Na_2O	0.13	0.12	0.15	0.15
K_2O	1.67	0.35	0.40	0.39
Total	94.69	91.02	91.15	90.85

Total bulk rock porosity: $7.6 \pm 3.2\%$ (n = 11)

I) The mobilized fraction of an element is equal to the difference of concentrations in bulk rock and red host rock normalized to the bulk rock concentration:

$$M = \frac{C_B - C_R}{C_B} \quad (1)$$

II) The mobilized fraction of an element is equal to the amount accumulated in the reduction spheres (bleached zones + cores) divided by the concentration in the bulk rock:

$$M = \frac{V_H (C_H - C_B) + V_C (C_C - C_B)}{C_B} \quad (2)$$

C_B = bulk rock concentration, C_R = concentration in red host rock,
C_H = concentration in bleached halo, C_C = concentration in cores,
V_H = volume fraction of haloes, V_C = volume fraction of cores,
M = mobile fraction of element.

With the two methods, the following results were obtained for the Kaisten 229 m section (percentage of elements mobilized from bulk rock during reduction sphere formation):

	(1)	(2)
As	27.5%	16.7%
U	17.7%	14.0%
Ni	12.2%	3.7%
V	6.5%	5.9%
Cu	--	4.8%

Lead is also strongly enriched in the cores, but depleted in the bleached zones by 43% relative to the red zones. This indicates that lead has been released during iron oxide/hydroxide dissolution. For other elements enriched in sphere cores, less than 1% of the total amount present in the rock is needed to explain the accumulations in the cores. Compared with leaching experiments carried out by ZIELINSKI et al. (1983) on Holocene-Pliocene red beds, the mobilities needed to explain element accumulations in spheres are lower than the experimentally derived mobile fractions except for Pb.

The V-content in sphere cores obtained by direct microprobe analysis (7.5% V_2O_3) is much higher than the XRF-derived content (1.5% V_2O_3). This is due to the fact that the XRF-sample containes less mineralized outer core parts while the microprobe analyses were performed on highly mineralized cores.

Results for reduction spheres from radiolarian cherts of Oman (Table 9) show a similar enrichment of V_2O_3 and, additionally, enrichments of K, Mg and Al in the core due to the formation of roscoelite. Mobility of K, Mg and Al could not be ascertained for the red bed samples because of the high background contents of these elements.

Comparing the mean concentrations in reduction sphere containing red beds with mineralogically similar, organic-rich lacustrine sediments from the Autunian of Weiach (1'214-1'343 m, 25-150 m below the red beds), there are some striking dissimilarities. The major element concentrations differ mainly in the lower oxidation state of iron in the Autunian. Differences in Al- and K-content are due to the predominance of kaolinite in the Autunian and of illite in the red beds. Most striking is the strong enrichment of As and B in the red beds compared with the underlying Autunian. Both elements are typically enriched in hydrothermally altered crystalline rocks in the potential source rock areas in Northern Switzerland (PETERS et al. 1987) and in the Black Forest (HOFMANN 1988). A plot of arsenic versus depth in Weiach (Fig. 6) clearly shows that the increase of As coincides with the appearance of red beds. There are three possible interpretations: I) The source area may have become more As-rich with the appearance of the red beds due to hydrothermal alteration. II) During the sedimentation of the organic-rich Autunian sediments, a mechanism removed As from the clastic material (biological methylation?). III) The iron oxyhydroxides present in the red beds provoked a syndepositional to diagenetic enrichement of arsenic.

7.2 Oxidation state of iron in reduction spheres

DURRANCE et al. (1978) performed investigations on the oxidation state of iron in reduction spheres from South Devon. They found increased levels of FeO in the spheres and concluded, that they had never been reddened. In the spheres from Kaisten, FeO is also slightly elevated compared with the red host rock. In order to determine the FeO-containing phase, FeO and CO_2 have been analyzed on clay fractions (< 2µm) and coarse fractions (> 63µm, depleted in clay) for three samples each of bleached and red zones from the Kaisten 229 m section. Both the clay- and the coarse fractions were depleted in FeO (wt.-%: red clay 0.56±0.04, bleached clay 0.62±0.07, red coarse 0.69±0.06, bleached coarse 0.65±0.05). CO_2 is enriched in the coarse and depleted in the clay fraction. Carbonate-rich fracture fillings postdating reduction sphere formation contained 1.70% FeO. These results show that carbonate is not a significant FeO-carrier in the bulk rock. Only about 5% of the total FeO can be in carbonates if the FeO-content of the fracture carbonate is taken as representative. FeO may be concentrated in the intermediate-size sheet silicates. Although the concentration of FeO is slightly elevated in the clay fractions of bleached zones than in the clays of the red host rock, it is not

possible to decide whether this is an inherited feature indicating that the spheres never were reddened (DURRANCE et al. 1978) or whether this is a secondary effect due to the formation of the reduction sphere in an already thoroughly reddened sediment.

7.3 Conclusions from the geochemical investigations:

- Hematite is quantitatively leached during red bed bleaching

- The bleached zones are slightly enriched in FeO

- Using the available geochemical and mineralogical information, reduction spheres can be shown to contain accumulations of C, Mg, Al, P, S, K, V, Cr, Co, Ni, Cu, Zn, As, Se, Y, Pd, Ag, Sb, Te, REE, Pt, Au, Hg, Tl, Pb, Bi, U. The association of elements accumulated varies from one site to the other. Only V and U are accumulated at all sites. Ti, Zr, Hf, Ta and Th were immobile.

- During reduction sphere formation, 5 to 30% of the elements As, U, Ni and V present in the bulk rock have been mobilized. For most other elements, a mobilization of less than 1% of the amount present in the bulk rock is needed.

- The red beds containing reduction spheres are strongly enriched in As and B compared with underlying, organic-rich Autunian sediments.

8 AGE OF REDUCTION SPHERE FORMATION

8.1 "Compaction age"

As evidenced by the shape of spheres, they have suffered a maximum of 20 to 26% compaction after formation. With the actual porosity of 11% (Kaisten), an original maximum porosity of 31 to 37% during sphere formation can be deduced. This yields a minimum depth of burial during formation and, thus, a maximum age. Using Figure 17 in RIEKE & CHILINGARIAN (1974), a depth of 500 to 1'000 m is obtained corresponding to Lower Dogger to Upper Malm or a maximum age of 175 to 140 m.y.

8.2 K/Ar-dating of roscoelite

K/Ar-dating was done on three nearly pure roscoelite separates from Riniken. The samples are from irregularly bleached zones which are thought to be contemporaneous with sphere formation. Microprobe analyses of the samples are presented on Table 4. Sample Rin 1032/2 contains some admixed illite and quartz, the other samples were pure roscoelites (XRD). The K/Ar-results are presented on Table 10.

The three ages obtained vary from Lower Jurassic to Lower Cretaceous. As roscoelite has not been used for dating purposes before, not much is known about argon retention of this mineral. The effect of argon overpressure during mineral formation is considered unimportant in this diagenetic environment. Because the samples weree not affected by metamorphism or oxidation and because the roscoelites are well crystallized sheet silicates, the ages obtained are interpreted as crystallization ages.

8.3 Microprobe U/Pb-ages

Chemical Pb/U-ratios are usually not regarded as good age indicators because of the possibility of element losses and the presence of nonradiogenic Pb. Ages of magmatic uraninites obtained by microprobe analysis generally are identical within the error with known intrusion ages of host granites (HOFMANN 1988). Because of the very fine grained nature of the U-phases in reduction spheres and their intergrowth with Pb-minerals like clausthalite, conventional U/Pb-dating would be difficult. Ages calculated from microprobe analyses are given on Table 11. Although the errors (based on the standard deviation of Pb/U-ratios of individual analyses) are quite large, three samples of first-generation U-phases yield a similar age of about 135 m.y. (Early Cretaceous). These "ages" should, of course, only be regarded as rough estimates.

In reduction spheres and in irregularly reduced zones in Kaisten, several U-phases have been found with no detectable Pb (< 0.1%) indicating low Pb-retentivity in these phases or very young age (< 10 m.y.).

8.4 Interpretation of obtained ages

The ages obtained by different methods show a considerable scatter, but are consistent so far as they indicate that reduction sphere formation occurred during the Mesozoic between 110 and 190 m.y. Reduction spheres, therefore, are late diagenetic and formed at depths of burial of 500 to 1'100 m. The presence of probably very young U-phases at Kaisten is an indication that element accumulation in reduction spheres might be episodic. The hypothesis of a very young age of some uranium phases in Kaisten is supported by U-series disequilibrium investigations (HOFMANN et. al. 1987) which indicate minor recent U accumulation at the edge of reduction spheres at Kaisten (230.0 m).

Table 10: K/Ar ages of roscoelites

Sample	C (1)	%K	%$40Ar_{rad}$	$40Ar_{rad}$ (2)	age m.y.(3)
Rin 1032/2	0.52	6.64	98.48	2.0959	173 ± 2
Rin 1068	0.35	7.54	98.73	1.5042	112 ± 2
Rin 1769/2	0.35	6.51	99.10	2.2610	190 ± 2

(1) crystallinity, half-width of 001-peak in °2 Θ

(2) 10^{-9} mol/g
(3) 1s-error

Table 11: Microprobe U/Pb-ages of uranium minerals

Sample	mineral	n	Pb/U(at)	age m.y.
Wef 245	pitchblende	5	0.0186 ±0.0110	113 ±67
Rin 1639 P	pitchblende	6	0.0220 ±0.0040	135 ±25
Rin 1639 B	brannerite	6	0.0156 ±0.0049	96 ±30
Wei 1076	pitchblende	8	0.0225 ±0.0020	138 ±12
Kai 230	coffinite	31	0.0166 ±0.0070	101 ±42
Kai 129	U-As-phase	6	<0.002	<12
Kai 351	U-As-phase	8	<0.002	<12

9 FLUID INCLUSIONS

Microthermometric measurements of fluid inclusions have been attempted in dolomite nodules with bleached spheres and ore minerals (Rin 910.80) and in calcite crystals with the same chemistry as calcite intimately associated with ore minerals in reduction spheres (Kai 227.10). The fluid inclusions were small (< 10μm) and most probably of primary origin (at least in the Riniken sample). The following results were obtained:

Rin 910.80 dolomite

melting point of ice: -20.5±3.5°C (-16.4 to -25.4°C, n = 8)
homogenization temperature: 86, 92, 103°C

Kai 227.10 calcite

melting point of ice: -16.5±4.0°C (-9.0 to -19.6°C, n = 8)
homogenization temperature: 77, 80°C

The trapped fluids are highly saline, probably of the Na-Ca-Cl-type. Highly saline fluids are widespread in postvaristic mineralizations in Europe and are believed to originate in the permocarboniferous basins (BEHR et al. 1987, BEHR & GERLER 1987). Only a few homogenization temperatures could be obtained, because of leakage. Not knowing the methane content, the pressure correction to apply is up to 40°C (POTTER 1977, MULLIS 1987) resulting in formation temperatures of 80 to 140°C.

Assuming a geothermal gradient of 30°C/km and a surface temperature of 20°C during the Mesozoic, a probably more realistic formation temperature for reduction spheres of 35 to 55°C is obtained.

10 GENESIS OF REDUCTION SPHERES

10.1 General model

The formation of reduction spheres is due to a geochemical process that operated at isolated sites in oxidized, hematitic rocks. Iron oxide was dissolved in the vicinity of a reductant and ore minerals containing a broad suite of rare elements were precipitated. The precipitation of ore minerals can be explained by the reduction of mobile, higher valence ions of V, U, As, S, Se, Te, Cr, Ag, Au, Cu, Bi, Pd and Sb and the combination of reduced species of these elements with Ni, Co, Pb and Zn to form ore minerals. Hematite has been dissolved in the spheres by reduction to ferrous iron or by (organic?) complexation of ferric iron. Because of the spherical shape of reduction spheres and the very small poresize of the host rock, element migration during the formation of reduction spheres must have occurred by diffusion of ions in the porewater.

Local precipitation of elements from the porewater led to the build-up of a concentration gradient and to diffusive element migration into what later became the core of the reduction sphere. Fe was dissolved in the sphere and high local Fe-concentrations provoked an outward diffusion of this element. High salinities of the porewater and a high redox potential in the host red bed may have enhanced the mobility of elements. Many of the elements concentrated in the sphere cores are mobile under oxidizing, high salinity conditions only, e.g. the noble metals Ag, Au, Pd and Pt (FUCHS & ROSE 1974, BOWLES 1986). The origin of the elements carried in the porewater can be explained by release from iron hydroxides during their alteration to hematite. This could have happened at any depth of burial because the temperature of the goethite-hematite transition is dependent on grain size effects and water activity (LANGMUIR 1971). Hematite can form near the surface and has been shown to be present in Pliocene sediments (ZIELINSKI et al. 1983). On the other hand, goethite is abundantly present in Mesozoic iron oolithes at depth exceeding 1 km in Northern Switzerland.

10.2 Amount of organic matter needed for sphere formation

Reduced carbon has a reduction capacity of 330 meq/g or approximately 333 meq/cm³. Typical core material contains 5% V_2O_3 (microprobe analyses). The formation of core material (reduction of V^{5+} to V^{3+} considered only) roughly consumed 3.5 meq/cm³ electrons (rock density 2.6 g/cm³). In the bleached zones at Kaisten, 3.8% hematite was dissolved, consumimg 1.14 meq/cm³ reducing capacity (rock density 2.4 g/cm³).

The volume ratios sphere/core range from < 10 to > 1'000. Taking a typical value of 250 for Kaisten spheres, the total reducing capacity

(assumed to have been concentrated in the core initially) must have been 288.5 meq/cm³. This would mean that the core initially contained about 87 vol.-% carbon (density 1 g/cm³). This is impossible, because porosity during sphere formation was only about 30 vol.-%. If hematite was dissolved as an organic ferric iron complex, even more organic matter would have been consumed. Since there is not enough space in the core for the amount of organic matter needed for reduction sphere formation, it must be concluded that the accumulation of organic matter in the core and its oxidation leading to ore mineral precipitation must have been synchronous or alternating.

Similar calculations were performed by HARTMANN (1963) for reduction spheres from Saxony. He found that 20 wt.-% organic matter were needed in the core. This corresponds to about 50 vol.-% and the same conclusions must be drawn as in the case of Northern Switzerland.

10.3 Origin of layered sphere cores

The layering in reduction spheres has been interpreted as Liesegang rings (LIESEGANG 1913) by several authors (PERUTZ 1940, EICHHOFF & REINECK 1952, HARRISON 1975). Liesegang rings are produced by counterdiffusion of species forming an insoluble compound by reaction. The rings are the result of local supersaturation at subsequently different sites. Alternatively, the layering in the cores of reduction spheres can be explained as the result of growth of the cores under slightly changing conditions giving way to the formation of successive mineral layers at the edge of the cores. Several arguments are in favor of the second interpretation:

I. Different Liesegang rings should be composed of the same mineral. In the cores, single layers are made up of several minerals and successive layers are mineralogically distinct.

II. Mineral precipitation greatly reduces the porosity of the cores. It seems most likely that organic matter accumulation and -oxidation occurred at the rim of the cores.

The layering in the cores is interpreted as a growth feature similar to growth patterns isotopically recorded in diagenetic carbonate concretions (RAISWELL 1987). The presence of a superposition of growth banding and Liesegang rings cannot be ruled out, however.

10.4 Nature of the reductant

The reductant (electron donor) leading to the formation of reduction spheres most probably was organic matter having a redox capacity of roughly 330 meq/g (pure C). Another possible candidate is detrital

pyrite, but this can be excluded because there are no remnants of pyrites of the required size and it is unlikely that pyrite would have survived early red bed diagenesis. Organic matter is preserved in the cores of reduction spheres in some cases, and in N Texas (PIERCE et al. 1964) and SW Oklahoma (CURIALE et al. 1983) organic matter is the main constituent of sphere cores. Organic matter causing reduction sphere formation cannot be of detrital origin as assumed by most authors, because:

- Reduction spheres also occur in crystalline rocks (e.g. lamprophyre dykes) and inside pebbles of crystalline rocks in red beds in the Riniken well and in Scotland (MAW 1868, plate 12, Fig. 14).

- Large reduction spheres occurring in S Devon (UK) needed at least 7.7 g of organic C for their formation. Nicely preserved sedimentary structures in the cores exclude the former presence of an organic fragment of a few cm size however.

- Detrital organic fragments would not be randomly distributed in the sediment as are reduction spheres are. Mudstones would contain smaller particles than sandstones and this would be reflected in the sphere size.

- Large reduction spheres often have layered cores with an innermost core nucleus only 1 mm in diameter. Such cores cannot have formed around a detrital particle large enough to provide the needed reduction capacity.

- It is highly unlikely that organic matter would have survived early diagenesis without being oxidized in a red bed.

It is concluded that the organic matter that caused reduction sphere formation must have accumulated at the site of the present core just like the other elements. This is the only way that the formation of very large spheres with embryonic cores of 1 mm diameter can be explained.

10.5 Possible cause of reduction sphere formation

It has been estimated that the probable formation temperatures were 35 to 55°C. Sulfides present in the sphere cores must have formed due to the in situ reduction of sulfate present in the porewater. This is evidenced by the presence of occasional anhydrite crystals in reduction sphere cores being replaced by sulfides (Kai 95.74). Sulfate reduction at temperatures of 35 to 55°C is reported to be possible only by bacterial activity (TRUDINGER 1985, MACHEL 1987). KROUSE et al. (1988) report chemical and isotopic evidence for thermochemical sulfate reduction at 90 to 175°C. This is, however, only possible if

hydrogen sulfide is initially present as a catalyst (ORR 1982). Both the temperature needed and the initial presence of hydrogen sulfide are prerequesites unlikely to be fulfilled in the case of reduction sphere formation in red beds. Sulfate reduction by microbiological activity seems more likely. The same probably applies for arsenic, which is not reduced abiologically in geochemical environments below 100°C (SCHAUFELBERGER 1988). Fungi and bacteria are able to reduce arsenite to arsine and methylated arsenic (KONETZKA 1977). Bacterial reduction of many of the elements present in reduction sphere cores (V, U, Bi, Se, Te) has been reported (KONETZKA 1977, JONES et al. 1984). It is possible that reduction sphere formation is the result of the activity of isolated populations of microorganisms in a diagenetic environment. If microorganisms are involved in reduction sphere formation, several questions arise:

- How did microorganisms get into the deep environment?

- What are their sources of energy and of carbon and what is their terminal electron aceptor?

In the cores of reduction spheres, concentric ore mineral structures of possible biological origin have been observed outlined by uraninite (Fig. 10 F) and niccolite. These structures might be interpreted as mineralized bacterial cell walls as they are similar in shape and size to experimentally mineralized bacterial cells (BUBELA & CLOUD 1983, BEVERIDGE & FYFE 1985).

10.6 Other genetic models

Early genetic models for reduction sphere formation relied on the reducing capacity of tri- and tetravalent vanadium present in the cores (SCHREITER 1929, EICHHOFF & REINECK 1952, MEMPEL 1960) or on the radioactivity of the cores (SCHREITER 1929, PERUTZ 1940). Since the elements accumulated are the result of the reduction sphere formation process, they cannot have caused this process.

Several authors explain reduction sphere formation by the reducing capacity of detrital organic matter (HARTMANN 1963, VAN DE POLL & SUTHERLAND 1976, DURRANCE et al. 1978, MYAKURA & HAMPTON 1984). As demonstrated, this is not a possible explanation for the formation of typical reduction spheres.

MEMPEL (1960), HARRISON (1975) and PARNELL (1985) note that reduction spheres have not formed around detrital particles but do not offer an explanation for the presence of the reductant.

PARNELL & EAKIN (1987) explain reduction sphere formation in Scotland as a result of leaking hydrocarbon reservoirs. The N Texas (PIERCE et

al. 1964) and SW Oklahoma (CURIALE et al. 1983) occurrences are spatially linked with hydrocarbon reservoirs and the organic matter causing reduction sphere formation is interpreted to be migrated hydrocarbons. No explanation is given for the formation of the nodular concretions of this organic matter in red beds, however. Concerning the origin of accumulated rare elements, some authors advocate a far distance hydrothermal origin (MEMPEL 1960, HARRISON 1975, JOHAN & POVONDRA 1987), but most agree with a local mobilization of the elements from the host-rock and transport in local ground- and porewaters (HARTMANN 1963, PIERCE et al. 1964, VAN DE POLL & SUTHERLAND 1976, DURRANCE et al. 1978, CURIALE et al. 1983).

It is obvious that no comprehensive genetic model exists which could explain the observed features. Most difficult to explain is the origin of the reductant and the cause for its reaction with dissolved rare elements at discrete, isolated sites in quite homogeneous rocks. The occurrence of reduction spheres is not restricted to a specific depositional environment, and spheres may be hosted by all kinds of oxidized, hematitic rocks.

11 RELEVANCE TO THE GEOCHEMISTRY OF RADIOACTIVE WASTE REPOSITORIES

11.1 Recent mobility of uranium and daughter elements in reduction spheres

Alpha spectrometric investigations on the state of equilibrium between ^{238}U, ^{232}Th and their respective daughter elements have been carried out in collaboration with AERE Harwell and have been presented elsewhere (HOFMANN et al. 1987). In the following, a summary of this work is given.

In two reduction spheres from Kaisten (depth 230.00 m), detailed sampling was done across the core, the bleached halo into the red host rocks. A total of 5 samples from the center of the two cores, 7 from the core margin, 9 from the bleached haloes and 6 from the red host rock were investigated by alphaspectrometry. Additionally, 3 samples of bulk rocks were investigated. The sample size ranged from a few mg (cores) to a few 100 mg. The samples were analyzed for ^{238}U, ^{234}U, ^{232}Th, ^{230}Th and ^{228}Th. The bulk rocks were found to be in radioactive equilibrium for all measured radionuclides. The significant disequilibria were found at the edge of the cores, only, with $^{234}U/^{238}U$ = 1.17±0.04 and $^{230}Th/^{234}U$ = 0.78±0.03. Surprisingly, the $^{228}Th/^{232}Th$ activity ratio was significantly below 1 at the edge of the cores (0.84±0.04) and in the bleached haloes (0.81±0.03), indicating loss of ^{228}Ra (half life 5.75 y).

The uranium and thorium concentrations of the bulk rock as determined by alphaspectroscopy (U: 7.08±0.17 ppm and Th: 16.11±0.24 ppm) compare well with the XRF determined values of this study (7.9 ±0.6 and 17.5±0.6 ppm).

11.2 Qualitative conclusions

From the study of reduction spheres, qualitative conclusions can be drawn which may be relevant for the safetey assessment of radioactive waste repositories, since there are several similarities between reduction spheres and radioactive waste repositories. These are:

- Reduction spheres and radioactive waste repositories represent high-concentration accumulations of certain rare elements in an environment with negligible or low concentrations of these elements; thus, high concentrations gradients occur at the edge of the element accumulations which may lead to a possible redistribution of elements.

- The host rocks of reduction spheres (red beds) are similar to possible host rocks of radioactive waste repositories in terms of

bulk mineralogy (illite clay, quartz, feldspars, carbonates) and permeability (mostly very low). Element migrations is therefore expected to be mostly diffusive. The oxidizing (hematite) red bed environment simulates radiolytically induced oxidizing conditions which may be encountered near high-level radioactive waste.

- Reduction spheres were formed and persisted at depths similar to the proposed burial depth of high-level radioactive waste repositories (about 1 km).

- Among the elements accumulated in the cores of reduction spheres are many of which are direct or chemical analogues for the elements present in radioactive waste: U, Th and their daughter elements, rare earth elements, selenium, palladium.

The following qualitative conclusions can be drawn from the investigations of reduction spheres:

- Under red-bed diagenetic conditions (fO_2 > hematite-magnetite, T < 100°C), at least the following analogue-relevant elements are quite mobile: U, REE, Se, Pd. Diffusive mobility of these elements over distances of centimeters to decimeters is evidenced by their accumulation in the center of the reduction spheres. Th is less mobile than the REE as practically no ^{232}Th-enrichment was observed. Presently, diffusion rates of these elements can not be quantitatively described using reduction spheres.

- Very locally (in the order of cm^3) persisting reducing conditions caused immobilization of U, REE, Se, Pd and many other elements due to the formation of ore minerals containing element(s) in a reduced state.

- It is not unlikely that microorganisms caused the reduction and immobilization of elements.

- The very local accumulation of reduced elements in the centers of reduction spheres persisted for roughly 10^8 years despite the generally oxidizing conditions (fO_2 > hematite-magnetite) and the steep concentration gradients.

- Uranium series disequilibrium investigations show that some uranium has been recently accumulated at the edge of the centers of reduction spheres in Kaisten. This demonstrates that there is a potential for investigations of recent radionuclide migration in reduction spheres. No evidence for migration of U from the highly enriched cores into the hematitic host rock has been found.

12. REFERENCES

BASHAM, I. R. & EASTERBROOK, G.D. 1977: Alpha-particle autoradiography of geological specimens by use of cellulose nitrate detectors.- Trans. Instn. Min. Metall. 86, sec. B, 96-98.

BEHR, H.-J. & GERLER, J. 1987: Inclusions of sedimentary brines in post-variscan mineralizations in the Federal Republic of Germany - a study by neutron activation analysis.- Chem. Geol. 61, 65-77.

BEHR, H.-J., HORN, E.E., FRENTZEL-BEYME, K. & REUTEL, CHR. 1987: Fluid inclusion characteristics of the variscan and post-variscan mineralizing fluids in the FRG.- Chem. Geol. 61, 273-285.

BEUTNER, E.C., & CHARLES, E.G. 1985: Large volume loss during cleavage formation, Hamburg sequence, Pennsylvania.- Geology 13, 803-805.

BEVERIDGE, T.J. & FYFE, W.S. 1985: Metal fixation by bacterial cell walls.- Canad. J. Earth Sci. 22, 1893-1898.

BOWLES, J.F.W. 1986: The development of platinum-group minerals in laterites.- Econ. Geol. 81, 1278-1285.

BUBELA, B. & CLOUD, P. 1983: Sulphide mineralization of microbial cells.- J. Austral. Geol. and Geophys. 8, 355-357.

CABRI, L.J. & TRAILL, R.J. 1966: New palladium minerals from Noril'sk, Western Siberia.- Canad. Mineralogist 8, 541-550.

CARTER, G.E.L. 1931: An occurrence of vanadiferous nodules in the Permian beds of South Devon.- Mineral. Mag. 22, 609-613.

CATHELINEAU, M., CUNEY, M., LEROY, J., LHOTE, F., NGUYEN-TRUNG, C., PAGEL, M. & POTY, B. 1982: Caractères minéralogiques des pechblendes de la province hercynienne d'europe.- In: Vein type and similar uranium deposits in rocks younger than proterozoic: Vienna, International Atomic Energy Agency IAEA-TC-295/21, 159-177.

CURIALE, J.A., BLOCH, S., RAFALSKA-BLOCH, J. & HARRISON, W. E. 1983: Petroleum-related origin for unraniferous organic-rich nodules of southwestern Oklahoma.- Bull. amer. Assoc. Petroleum Geol. 67, 588-608.

DALE, T.N. 1899: The slate belt of eastern New York and western Vermont.- Ann. Rept. U.S. Geol. Surv., No. 19, part 3, 153-307.

DIEBOLD, P. 1987: Geologische Resultate der reflexionsseismischen Untersuchungen der Nagra in der Nordschweiz.- Nagra informiert 9, Nr. 1+2, 23-33.

DURRANCE, E.M., MEADS, R.E., BALLARD, R.R.B. & WALSH, J.N. 1978: Oxidation state of iron in the Littleham Mudstone Formation of the New Red Sandstone Series (Permian-Triassic) of southeast Devon, England.- Bull. geol. Soc. Amer. 89, 1231-1240.

DYCK, W. & McCORKELL, R.H. (1983): A study of uranium-rich reduction spheroids in sandstones from Pugwash Harbour, Nova Scotia.- Canad. J. Earth Sci. 20, 1738-1746.

EICHHOFF, H.J. & REINECK, H.E. 1952: Uran-Vanadiumkerne mit Verfärbungshöfen in Gesteinen.- N. Jb. Mineral. Abh. 11/12, 294-314.

ELLSWORTH, H.V. 1928: Thucholite, a remarkable primary carbon mineral from the vicinity of Parry Sound, Ontario.- Amer. Mineralogist 13, 419-439.

FESSER, H. 1971: Kupfer-Mineralien auf Helgoland.- Aufschluss 22, 221-225.

FLISCH, M. 1982: Potassium-argon analysis.- In: Odin, G.S., ed., Numerical Dating in Stratigraphy, John Wiley, Chichester, 151-158.

FOSTER, M.D. (1959): Chemical study of the mineralized clays.- In: Geochemistry and Mineralogy of the Colorado Plateau Uranium ores. Prof. Pap. U.S. geol. Surv. 320, 121-132.

FREY, M., TROMMSDORFF, V. & WENK, E. 1980: Alpine metamorphism in the central Alps.- Excursion VI In: Geology of Switzerland, a guidebook, Wepf and Co, Basel and New York, 295-316.

FUCHS, W.A. & ROSE, A.W. 1974: The geochemical behaviour of platinum and palladium in the weathering cycle in the Stillwater Complex, Montana: Econ. Geol. 69, 332-346.

GRIP, E. & ÖDMANN, O.H. 1944: On Thucholite and natural gas from Boliden.- Sveriges geol. Unders. Ser. C, 464, 3-19.

HARRISON, R.K. 1975: Concretionary concentrations of the rarer elements in Permo-Triassic red beds of South-West England.- Bull. geol. Surv. G.B. 52, 1-26.

HARTMANN, M. 1963: Einige geochemische Untersuchungen an Sandsteinen aus Perm und Trias.- Geochim cosmochim. Acta 27, 459-499.

HILL, J. 1954: Uraniferous Asphaltic Materials of Southwestern Oklahoma.- Bull. geol. Soc. Amer. 65, 1377.

HOEVE, J. & SIBBALD, T.I.I. 1978: On the genesis of Rabbit Lake and other unconformity-type uranium deposits in northern Saskatchewan, Canada.- Econ. Geol. 73, 1450-1473.

HOFMANN, B. 1986: Small-scale multi-element accumulations in Permian red-beds of Northern Switzerland.- N. Jb. Mineral. Mh., Jg. 1986, 367-375.

HOFMANN, B. 1987: Die Erzmineralien.- In: Peters, Tj., Matter, A., Bläsi, H.-J. and Gautschi A., Sondierbohrung Böttstein - Geologie. Nagra Technical Report 85-02, Baden 133-140.

HOFMANN, B. 1988: Genese, Alteration und rezentes Fliess-System der Uranlagerstätte Krunkelbach (Menzenschwand, Südschwarzwald).- Nagra Technical Report 88-30, Baden, 195p.

HOFMANN, B., DEARLOVE, J.P.L., IVANOVICH, M., LEVER, D.A., GREEN, D.C., BAERTSCHI, P. & PETERS, TJ. 1987: Evidence of fossil and recent diffusive element migration in reduction haloes from Permian red-beds of Northern Switzerland.- In: Côme, B. and Chapman, N.A., eds., Natural analogues in radioactive waste disposal: Brussels and Luxembourg, Commission of the European Communities, 217-238.

JAMES, G.W. 1977: Parts-per-million determinations of uranium and thorium in geological samples by X-ray spectrometry.- Analyt. Chem. 49, No. 7, 967-969.

JOHAN, Z. & POVONDRA, P. 1987: Vanadium- and copper-bearing dolomite nodules from Permian sediments near Horni Kalna, Czechoslovakia.- N. Jb. Mineral. Abh. 157, 245-266.

JONES, J.G. DAVISON, W. & GARDENER, S. 1984: Iron reduction by bacteria: range of organisms involved and metals reduced.- FEMS Microbiology Letters 21, 133-136.

KONETZKA, W.A. 1977: Microbiology of metal transformations.- In: Weinberg, E.D., ed., Microorganisms and minerals. Marcel Dekker Inc., New York-Basel, 317-342.

KROUSE, H.R., VIAU, C.A., ELIUK, L.S., UEDA, A. & HALAS, S. 1988: Chemical and isotopic evidence of thermochemical sulphate reduction by light hydrocarbon gases in deep carbonate reservoirs.- Nature 333, 415-419.

KUCHA, H. 1982: Platinum-group metals in the Zechstein copper deposits, Poland: Econ. Geol. 77, 1578-1591.

KUCHA, H. 1984: Palladium minerals in the Zechstein copper deposits in Poland.- Chemie d. Erde, 43, 27-43.

KUCHA, H. 1988: Graphite in Kupferschiefer (Poland) and its genetic meaning.- Mineralium Depos. 23, 174-178.

LANGMUIR, D. 1971: Particle size effect on the reaction goethite = hematite + Water.- Amer. J. Sci. 271, 147-156.

LAUBSCHER, H. 1987: Die tektonische Entwicklung der Nordschweiz.- Eclogae geol. Helv. 80, 287-303.

LEVENTHAL, J.S., GRAUCH, R.I., THRELKELD, C.W., LICHTE, F.E. & HARPER, C.T. 1987: Unusual organic matter associated with uranium from the Claude Deposit, Cluff Lake, Canada.- Econ. Geol. 82, 1169-1176.

LIESEGANG, R.E. 1913: Geologische Diffusionen.- Dresden and Leipzig, Theodor Steinhopff Verlag, 180p.

MACHEL, H.G. 1987: Some aspects of diagenetic sulfate-hydrocarbon redox reactions.- In: Marshall, J.D., ed., Diagenesis of sedimentary sequences. Geol. Soc. Spec. Pub., No. 36, Blackwell Scientific Pub., Oxford, 15-28.

MATTER, A. 1987: Faciesanalyse und Ablagerungsmilieus des Permokarbons im Nordschweizer Trog.- Eclogae geol. Helv. 80, 345-367.

MATTER, A., PETERS, TJ., BLÄSI, H.-R., MEYER, J., ISCHI, H. & MEYER, CH. 1988: Sondierbohrung Weiach, Geologie.- Nagra Technical Report 86-01, Baden, 438p.

MATTER, A., PETERS, TJ., ISENSCHMID, CHR., BLÄSI, H.-R. & ZIEGLER, H.J. 1988: Sondierbohrung Riniken, Geologie.- Nagra Technical Report 86-02, Baden, 198p.

MAW. G. 1868: On the disposition of iron in variegated strata.- Quart. J. geol. Soc. London 24, 351-400.

MEMPEL, G. 1960: Neue Funde von Uran-Vanadiumkernen mit Entfärbungshöfen.- Geol. Rdschau. 49, 263-276.

MILLER, W.J. 1910: Origin of color in the Vernon shale.- Bull. New York State Mus. 140, 150-156.

MÜLLER, W.H., HUBER, M., ISLER, A. & KLEBOTH, P. 1984: Erläuterungen zur gelogischen Karte der zentralen Nordschweiz 1:100'000. Nagra Technical Report 84-25, Baden, 234p.

MULLIS, J. 1987: Fluideinschluss-Untersuchungen in den Nagra-Bohrungen der Nordschweiz.- Eclogae geol. Helv. 80, 553-568.

MYAKURA, H. & Hampton, B.P. (1984): On the mechanism of formation of reduction spots in the Carboniferous/Permian red beds of Warwickshire.- Geol. Mag. 121, 71-74.

ORR, W.L. 1982: Rate and mechanism of non-microbial sulfate reduction.- Abstr. north-amer. Geol., 1982, 580.

PARNELL, J. 1985: Uranium/rare earth-enriched hydrocarbons in Devonian sandstones, Northern Scotland.- N. Jb. Mineral. Mh., Jg. 1985 132-144.

PARNELL, J. 1988: The mineralogy of red bed uranium-vanadium mineralization in the Permo-Triassic of Belfast.- Irish J. Earth Sci. 10.

PARNELL, J. & EAKIN, P. 1987: The replacement of sandstones by uraniferous hydrocarbons; significance for petroleum migration.- Mineral. Mag. 51, 505-515.

PERCH-NIELSEN, K., BIRKENMAYER, T., BIRKELUND, T. & AELLEN, M. 1974: Revision of Triassic stratigraphy of the Scoresby Land and Jameson Land region, East Greenland.- Bull. Gronl. geol. Unders. 109, 51.

PERUTZ, M. 1940: Radioactive nodules from Devonshire, England.- Mineral. petrogr. Mitt. (Wien) 51, 141-161.

PETERS, TJ. 1987: Das Kristallin der Nordschweiz.- Petrographie und hydrothermale Umwandlungen: Eclogae geol. Helv. 80, 305-322.

PETERS, TJ., MATTER, A., BLÄSI, H.-R. & GAUTSCHI, A. 1987: Sondierbohrung Böttstein, Geologie.- Nagra Technical report 85-02, Baden, 207p.

PIERCE, A.P., GOTT, G.B. & MYTTON, J.W. 1964: Uranium and helium in the Panhandle Gas Field, Texas, and adjacent areas.- Prof. Pap. U.S. Geol. Surv. 454-G, 57.

PIERCE, A.P. & ROSHOLT, J.N. 1961: Radiation damage and isotopic disequilibria in some uranium-bearing asphaltite nodules in back-reef dolomite, Carlsbad, New Mexico.- Prof. Pap. U.S. Geol. Surv. 424-D, 320-323.

POLL, VAN DE, H.W. & SUTHERLAND, J.K. 1976: Cupriferous reduction spheres in Upper Mississippian redbeds of the Hopewell Group at Dorchester Cape, New Brunswick.- Canad. J. Earth Sci. 13, 781-789.

PONSFORD, D.R.A. 1954: Note on the occurrence of uranium in certain horizons in the Enville beds.- Bull. geol. Surv. G.B. 5, 59-61.

POTTER, R.W. 1977: Pressure corrections for fluid-inclusion homogenization temperatures based on the volumetric properties of the system NaCl-H_2O.- J. Res. U.S. Geol. Surv. 5, 603-607.

RAISWELL, R. (1987): Non-steady state microbiological diagenesis and the origin of concretions and nodular limestones.- In: Marshall, J.D., ed., Diagenesis of sedimentary sequences. Geol. Soc. London Spec. Publ. 36, 41-54.

RIEKE, H.H. & CHILINGARIAN, G.V. 1974: Compaction of argillaceous sediments.- Dev. Sedimentol. 16, 424.

SCHADE, J., OHNENSTETTER, D. & GIRAULT, J. 1986: Première découverte de roscoélite en France, dans le permien uranifère des Alpes. Intérêt métallogénétique de ce mica vanadifère.- C.R. Acad. Sci. (Paris) 302, série II, No. 7, 427-430.

SCHAUFELBERGER, F.A. (1988): Arsenides, genesis and extraction.- In: Reddy, R.G., Hendrix, J.L. and Querneau, P.B., eds., Arsenic Metallurgy, Fundamentals and Applications. The metallurgical Inc., society Inc., Phoenix, Jan. 25-27, 1988 (Proc.), 455-468.

SCHIDLOWSKI, M. 1981: Uraniferous constituents in the Witwatersrand conglomerates: Ore-microscopic observations and implications for the Witwatersrand metallogeny.- Prof. Pap. U.S. Geol. Surv. 1161, N1-N29.

SCHREITER, R. 1929: Zur Bleichung rotliegender Sedimente durch Vanadinverbindungen.- Z. dtsch. geol. Ges. 81, 293-294.

SCHREITER, R. 1930: Vanadinhaltige Kerne, Bleichungsringe und Bleichungszonen in den Schieferletten des Rotliegenden von Sachsen.- Z. dtsch. geol. Ges. 82, 41-47.

SCHREITER, R. 1932: Kupfererze im Buntsandstein von Helgoland.- Z. dtsch. geol. Ges. 84, 1-17.

SKOCEK, V. 1967: Vanadium and Uranium accumulations in the Permo-Carboniferous sediments of central and north-eastern Bohemia.- Cas. Mineral. Geol. 12, 419-424.

TANTON, T.L. 1948: Radioactive nodules in sediments of the Sibley Series, Nipigon, Ontario.- Trans. r. Soc. Can. 17, Ser. III, Sec. 4, 69-75.

TISCHENDORF, G. & UNGETHÜM, H. 1964: Über die Bildungsbedingungen von Clausthalit-Galenit und Bemerkungen zur Selenverteilung im Galenit in Abhängigkeit vom Redoxpotential und vom pH-Wert.- Chemie d. Erde 23, 279-311.

TRUDINGER, P.A., CHAMBERS, L.A. & SMITH, J.W. 1985: Low temperature sulfate reduction: biological versus abiological.- Canad. J. Earth Sci. 22, 1910-1918.

WEEKS, A.D., COLEMAN, R.G. & THOMPSON, M.E. 1959: Summary of the ore mineralogy.- Prof. Pap. U.S. geol. Surv. 320, 65-79.

WIENER, G. 1975: Ein Vorkommen von gediegenem Kupfer im Buntsandstein des Tafeljura (Kaiseraugst, Kt. Aargau).- Eclogae geol. Helv. 68, 229-237.

ZIELINSKI, R.A., BLOCH, S. & WALKER, T.R. (1983): The mobility and distribution of heavy metals during the formation of first cycle red beds.- Econ Geol. 78, 1574-1589.

Reduction spheres: Estimation of formation times

Peter Baertschi, Nagra

The time required for the formation of dark cores and bleached halos in reduction spheres has been tentatively calculated on the basis of the model of continuous diffusion of reactants to and from a reaction center as proposed by B. HOFMANN. Numerical results remain uncertain, however, since concentrations at the time of formation are unknown and only present day data are available.

1. Formation of dark cores

At some reaction centers, reduction of ore forming solute to form insoluble species takes place - either by some unknown chemical catalytic processes or by microbial activity. The concentration of the reactants thus drops to very low values in the groundwater at the margin of the growing cores.

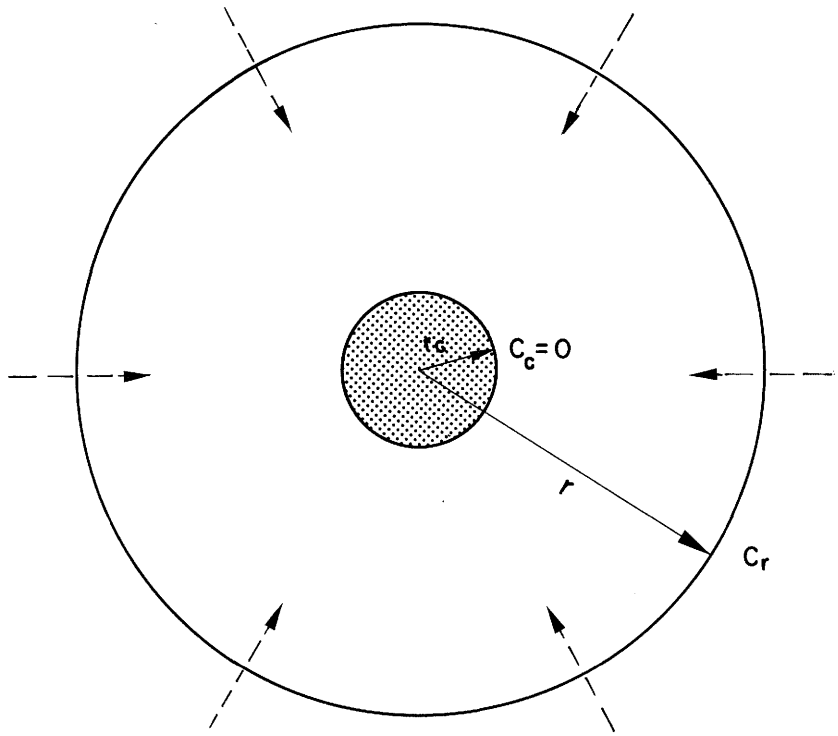

Figure 1: Growth of dark core by radial diffusion of reactants

simplifying assumptions:

- core homogeneous with radius r_c
- concentration $C_c = 0$ (at core margin r_c)
- C_∞ = const. (at distances $r >> r_c$)

According to Fick's law for stationary diffusion the transport rate, dQ/dt, becomes:

$$dQ/dt = 4\pi D \cdot C_\infty \cdot r_c \quad (1)$$

with the concentration $C_r = C_\infty (1 - r_c/r)$ (2)
as shown in Figure 2

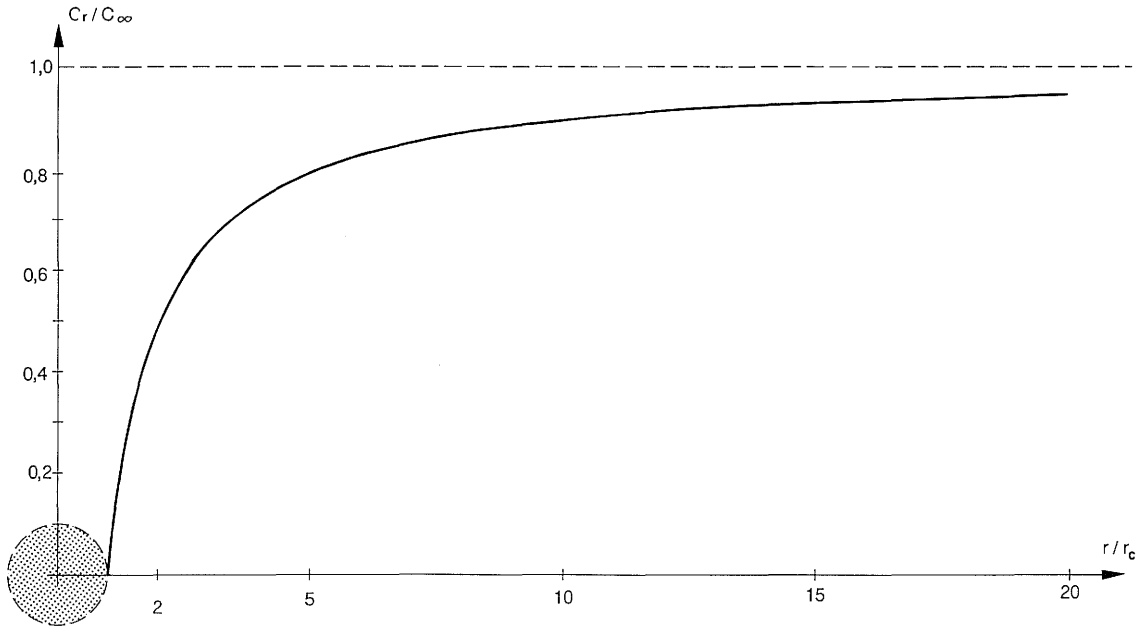

Figure 2: Concentration C_r (normalized as C_r/C_∞) as a function of r/r_c.

The diffusion coefficient of ions (simple and complex) in bulk water is, in general, rather close to 10^{-5} cm^2 s^{-1}. The same is true for small and medium size molecules, with the exception of H_2 (diffusing about 4 times faster). For red beds, with some 30% porosity and at somewhat elevated temperature (< 100°C), a diffusion coefficient D of 10^{-6} cm^2 s^{-1} ($4 \cdot 10^{-6}$cm^2 s^{-1} for H_2) is estimated.

1.1 Transport of ore forming ions

For an ore forming component i (e.g. uranium) the total accumulated quantity Q_i is

$$Q_i = (4 \pi r_c^3/3) \cdot \rho_c \cdot m_i \quad (3)$$

with ρ_c, density of core material (average)
m_i, mass fraction of component i in the core

From eq. (3) : $dQ_i/dr_c = 4 \pi \rho_c m_i r_c^2$ (4)

With $dQ_i/dt = dQ_i/dr_c \cdot dr_c/dt$, and eq (1) and (4), one obtains

$D_i C_{\infty i} = \rho_c m_i r_c (dr_c/dt)$ or $dt = (\rho_i m_i / D_i C_{\infty i}) r_c \cdot dr_c$

Integration gives the growth time of the core

$t = (r_c^2 \rho_c m_i)/2D_i C_{\infty i} = 3Q_i/(8\pi r_c D_i C_{\infty i}) \simeq Q_i/(8 r_c D_i C_{\infty i})$ (5)

Typical data for a reduction sphere (halo 1 in HOFMANN et al. (1987)) are:

$r_c = 0.4$ cm, $Q_U = 0.05$ g (uranium)

For Permian waters, uranium contents between 0.02 and 0.5 ppb have been found in the Nagra boreholes Weiach, Riniken and Kaisten (WITTWER 1986; PEARSON et al. 1989). A concentration of $C_U = 0.1$ ppb (10^{-10} g/g) may tentatively be taken as typical.

With $D_U = 10^{-6}$ cm^{2}s^{-1} eq (5) becomes:

$t = 0.05/(8 \cdot 0.4 \cdot 10^{-6} \cdot 10^{-10}) = 1.6 \cdot 10^{14}$s $= 5 \cdot 10^6$a

Lower formation times result with higher uranium concentrations, e.g. for $C_{U\infty} = 1$ ppb, $t = 5 \cdot 10^5$a.

Smaller cores develop faster. Since Q_i is roughly proportional to r_c^3, the time, t, goes with r_c^2 according to eq (5). A small core with $r_c = 0.04$ cm and a uranium inventory of $Q_U = 5 \cdot 10^{-4}$ g thus develops in $5 \cdot 10^4$a (with $C_{U\infty} = 0.1$ ppb).

Similar growth time calculations could also be done with vanadium which is highly enriched in the cores of most reduction spheres. Unfortunately, no vanadium contents in Permian waters of the Nagra boreholes have been measured, but from other sources a range of 0.1 to 1 ppb simmilar to uranium appears to be realistic. Since the inventory of vanadium in the cores is comparable to that of uranium, growth times of the same order of magnitude could be calculated.

1.2 Transport of reductants, necessary for ore formation

Eq (5) also applies to the radial transport of dissolved primary reductants such as H_2, CH_4, CH_3COOH, NH_3.

For the formation of a reduction sphere with $r_c = 0.4$ cm (0.27 cm^3) and a halo-radius $r_h = 2$ cm (34 cm^3) HOFMANN estimates the following requirements for reducing capacity:

core	3.5 meq/cm^3	-->	1 meq	
halo	1 meq/cm^3	-->	34 meq	35 meq (total)

The maximum reducing capacities of some possible natural reductants observed in present day permian groundwaters and the corresponding amounts needed for the sphere build up are:

Reductant and oxidation products	Reducing capacity (max)	Amount necessary for 35 meq (red. sphere)
H_2 (--> H_2O)	2 eq/mol = 1 meq/mg	0.035 g
CH_4 (--> CO_2+$2H_2O$)	8 eq/mol = 0.5 meq/mg	0.07
CH_3COOH (--> $2CO_2$+$2H_2O$)	8 eq/mol = 0.13 meq/mg	0.26
NH_3 (--> NO_3^-+3/2 H_2O)	8 eq/mol = 0.5 meq/mg	0.07

Concentrations C_∞ of H_2, CH_4 and NH_3 in Permian waters of the Nagra boreholes Weiach, Riniken and Kaisten are reported by WITTWER (1986) and PEARSON et al. (1989). They vary over a wide range but, tentatively, 1 ppm for CH_4 and NH_3 and 0.1 ppm for H_2 can be considered as typical. Also, acetate may be present at the 1 ppm level.

With these concentrations C_∞, and with Cr = 0 at core margin and by accepting a diffusion coefficient of $D = 10^{-6}$ cm^2s^{-1} ($4 \cdot 10^{-6}$ for H_2) in the red bed eq (5) leads to the following accumulation times for the necessary amounts of reductants:

H_2, 900 a; CH_4, 700 a; NH_3, 700 a; CH_3COO^-, 2600 a

Actually, since the assumption of zero concentration at the core margin probably does not hold for these reductants, the accumulation times will be longer, but still much shorter than the accumulation times for the ore forming components. The proposed model of continuous supply of reductants during core formation thus appears to be very probable and, accordingly, the growth rate of the cores is determined rather by the availability of ore forming components in the groundwater than by that of dissolved reductants.

2. Formation of reduction halos
(bleached zone around core)

Proposed model: At the margin of the core at r_c a parallel reaction produces a secondary reductant, which - in contrast to the more inert primary reductants- is able to reduce Fe_2O_3 to FeO (e.g. $S_2O^{--}_4$, H_2S, organic compounds). Its concentration, C_c, at the core margin is assumed to be constant and it diffuses outward. As it meets the hematite (Fe_2O_3) at the halo radius, r_h, it is oxidized and thus vanishes: C_h=0. The reaction zone at the halo radius is sharp, as usually observed in reduction spheres, if the rate of Fe_2O_3-reduction is fast compared to the outward diffusion of the secondary reductant.

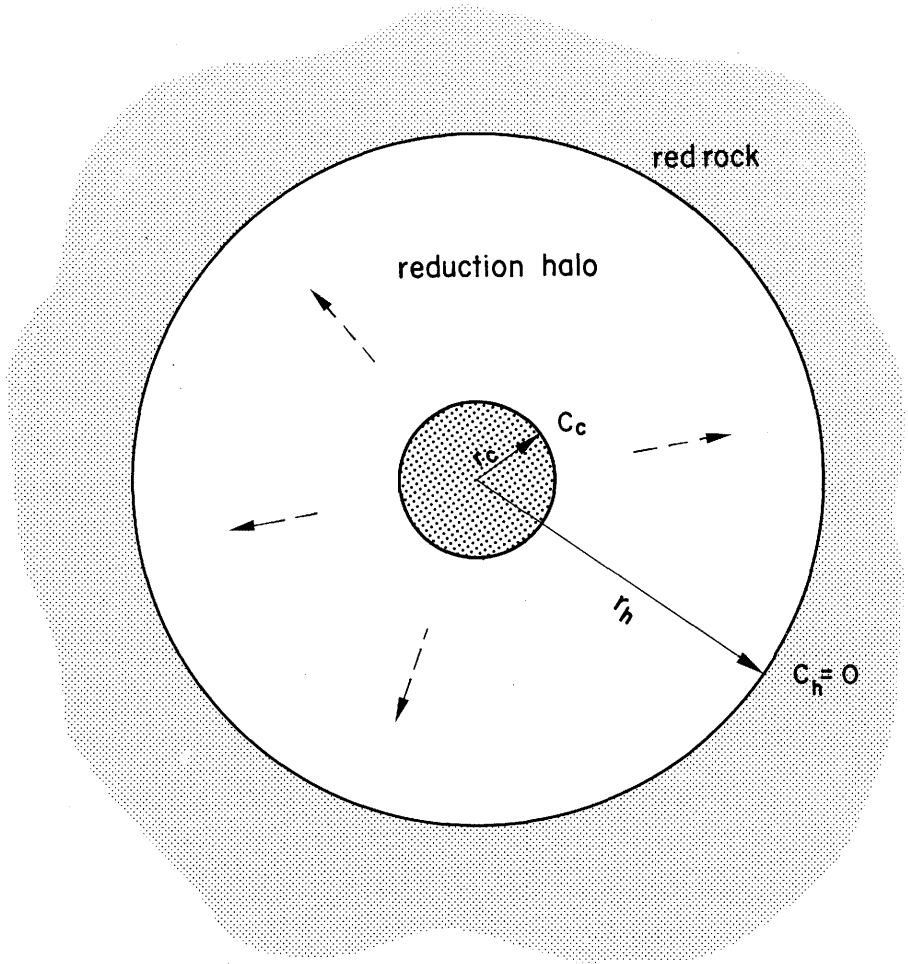

Figure 3: Growth of reduction halo by radial diffusion (outward) of secondary reductant.

Simplifying assumptions:

- core radius r_c remains constant during build up of halo.
- concentration of secondary reductant at core margin, C_c remains constant.

For a halo radius r_h, the stationary transport rate, dQ/dt, becomes:

$$dQ/dt = -4\pi Dr^2 (dC/dr) = \text{const} \quad (6)$$

integration between r_h and r_c leads to

$$dQ/dt = 4\pi D(C_c - C_h) r_h r_c / (r_h - r_c) \quad (7)$$

For $r_h \gg r_c$ and with $C_h = 0$, eq (7) is similar to eq (1) with C_c instead of C_∞ corresponding to the outward diffusion.

The concentration C_r for any radius r between the core margin r_c and the sphere radius r_h is

$$C_r = C_c\ ((r_h/r) - 1)r_c/(r_h - r_c) \qquad (8)$$

The growth of the bleached zone proceeds according to the rate of reduction of Fe_2O_3, as induced by the arriving reductant.

With m, amount of reductant (in meq), necessary to reduce 1 g of Fe_2O_3
g_F, mass fraction of Fe_2O_3 in the red rock
ρ , density of the red rock (gcm^{-3})

the necessary amount of reductant (meq) to move the front at r_h by dr becomes

$$dQ = m \cdot 4\pi r_h^2(dr) \cdot \rho \cdot g_F \quad \text{or} \quad r_h^2(dr) = dQ/(4\pi \rho \cdot g_F m)$$

Introducing dQ from eq (7) and omitting the suffix h in the growing halo radius r_h gives

$$(r(r - r_c)/r_c)dr = (C_c D/\rho \cdot g_F m)dt \qquad (9)$$

Integration between r_c and r_h leads to the growth time t

$$t = (r_h^3/3r_c - r_h^2/2 + r_c^2/6)(\rho \cdot g_F m)/C_c D \qquad (10)$$

typical data are: r_h = 2 cm, r_c = 0.4 cm, g_F = 0.06, ρ = 2.5 gcm^{-3}
m = 12.8 meq/g Fe_2O_3, D≈10^{-6} cm^2s^{-1}

It is very difficult to estimate C_c, the concentration of the secondary reductant at the core margin. This is a sink for all reactants in the porewater which are involved in the formation of the core. C_c is thus probably lower than the concentrations of primary reductants in the rock porewater. Tentatively, an order of magnitude of 10^{-6} meq/cm^3 may be assumed.

Introducing these data into eq (10), the formation time of the halo becomes

$$t \approx 3 \cdot 10^5 a$$

The much higher requiremenmt for reducing capacity for halo formation than for core build up (factor 34 in the example but highly variable in general) suggests that the reaction chain leading from the primary to the secondary reductant, and to hematite reduction in the halo, is the predominant process. The reduction of ions to the ore-like material of the dark core may be a side reaction.

3. Conclusions

a) The growth time of a reduction sphere of some 5 cm diameter with a core of about 1 cm diameter is of the order of 10^6 a assuming continuous growth and accepting present day concentrations of uranium in Permian groundwater.

b) Using present day concentrations of possible primary reductants in the groundwater, it is found that these would by far be sufficient to produce the reduction spheres around specific reaction centers.

c) The production of the secondary, outward diffusing reductant appears to be the main reaction at the core margin. The formation of core material proceeds at a lower rate and may thus be a side reaction.

d) In case of biogenic origin of the reduction processes, the slow growth of the reduction spheres would suggest a very low rate of microbial activity.

References:

- HOFMANN B., DEARLOVE J.P.L., IVANOVICH M., LEVER D.A., GREEN D.C., BAERTSCHI P. and PETERS TJ. 1987:
Evidence of fossil and recent diffusive element migration in reduction haloes from Permian red-beds of Northern Switzerland; in: Côme, B. and Chapman, N.A., eds., Natural Analogues in radioactive waste disposal. Commission of the European Communities, Brussels & Luxemburg, 217-238 (CEC Report EUR 11037 EN).

- WITTWER C. 1986
Probennahmen und chemische Analysen von Grundwässern aus den Sondierbohrungen. NAGRA NTB 85-49, Nagra Baden.

- PEARSON, F.J., Jr. LOLCAMA, J.L. and SCHOLTIS, A. 1989:
Chemistry of waters in the Böttstein, Weiach, Riniken, Schafisheim, Kaisten and Leuggern boreholes: A hydrochemically consistent data set. NAGRA NTB 86-19, Nagra, Baden, Switzerland